SPECTRAL WHITENING WITH APPLICATION TO EXPLOSION P^{P}

T. J. Cohen, et al

Teledyne Geotech

Prepared for:

Advanced Research Projects Agency

12 January 1972

.....contributing to ...ne's
understanding of the environment world

SPECTRAL WHITENING WITH APPLICATION TO EXPLOSION pP

T. J. COHEN
R. L. SAX
H. L. HUSTED
SEISMIC DATA LABORATORY

12 JANUARY 1972

Prepared for
AIR FORCE TECHNICAL APPLICATIONS CENTER
Washington, D.C.

Under
Project VELA UNIFORM

Sponsored by
ADVANCED RESEARCH PROJECTS AGENCY
Nuclear Monitoring Research Office
ARPA Order No. 1714

TELEDYNE GEOTECH
ALEXANDRIA LABORATORIES

80

Unclassified

Security Classification

DOCUMENT CONTROL DATA · R&D

(Security classification of title, body of abstract and indexing annotation must be entered when the overall report is classified)

1. ORIGINATING ACTIVITY (Corporate author)
TELEDYNE GEOTECH
ALEXANDRIA, VIRGINIA

2a. REPORT SECURITY CLASSIFICATION
Unclassified

2b. GROUP

3. REPORT TITLE
SPECTRAL WHITENING WITH APPLICATION TO EXPLOSION pP

4. DESCRIPTIVE NOTES (Type of report and inclusive dates)
Scientific

5. AUTHOR(S) (Last name, first name, initial)
Cohen, T.J.;, Sax, R.L.; Husted, H.L.

6. REPORT DATE	7a. TOTAL NO. OF PAGES	7b. NO OF REFS
12 January 1972	~~78~~ 80	7

8a. CONTRACT OR GRANT NO.	9a. ORIGINATOR'S REPORT NUMBER(S)
F33657-72-C-0009	282
b. PROJECT NO. VELA T/2706	
c. ARPA Order No. 1714	9b. OTHER REPORT NO(S) (Any other numbers that may be assigned this report)
d. ARPA Program Code NO. 2F-10	

10. AVAILABILITY/LIMITATION NOTICES

APPROVED FOR PUBLIC RELEASE, DISTRIBUTION UNLIMITED.

11. SUPPLEMENTARY NOTES	12. SPONSORING MILITARY ACTIVITY
	Advanced Research Projects Agency Nuclear Monitoring Research Office Washington, D. C.

13. ABSTRACT

A method is proposed for whitening the spectra of teleseismic P waves to aid in the determination of event depths. The method uses a network of common recording stations, all of which must have recorded signals from a suite of closely-spaced events, e.g., a set of underground explosions. Individual spectra are whitened by removing a path-recording site response determined by averaging spectra from the suite of events as recorded at a single station. The whitened spectra from a single event are then summed over the recording network to yield a whitened source spectra. The whitening process enhances spectral components in the band 2 to 5 Hz. Application of the proposed whitening method to explosion spectra for theoretical and experimental data sets indicates that the method may be useful in analyzing spectral nulls provisionally interpreted as due to pP-P interference. Depth-phase anlaysis for seven NTS explosions, using both whitened and unwhitened data, shows that spectral nulls are enhanced in the whitened spectra. Network summed spectra (unwhitened) for seventeen earthquakes are also included; these demonstrate the fact that nulls can be caused, for example, by multipath effects and multiplet sources as well as by depth-phase interference.

14. KEY WORDS

Depth Phase
Spectral Whitening
pP
Spectral Analysis
Spalling

Unclassified

Security Classification

SPECTRAL WHITENING WITH APPLICATION TO EXPLOSION pP

SEISMIC DATA LABORATORY REPORT NO. 282

AFTAC Project No.:	VELA T/2706
Project Title:	Seismic Data Laboratory
ARPA Order No.:	1714
ARPA Program Code No.:	2F-10
Name of Contractor:	TELEDYNE GEOTECH
Contract No.:	F33657-72-C-0009
Date of Contract:	01 July 1971
Amount of Contract:	$ 1,314,000
Contract Expiration Date:	30 June 1972
Project Manager:	Royal A. Hartenberger (703) 836-7647

P. O. Box 334, Alexandria, Virginia

ib

ABSTRACT

A method is proposed for whitening the spectra of teleseismic P waves to aid in the determination of event depths. The method uses a network of common recording stations, all of which must have recorded signals from a suite of closely-spaced events, e.g., a set of underground explosions. Individual spectra are whitened by removing a path-recording site response determined by averaging spectra from the suite of events as recorded at a single station. The whitened spectra from a single event are then summed over the recording network to yield a whitened source spectra. The whitening process enhances spectral components in the band 2 to 5 Hz. Application of the proposed whitening method to explosion spectra for theoretical and experimental data sets indicates that the method may be useful in analyzing spectral nulls provisionally interpreted as due to pP-P interference. Depth-phase analysis for seven NTS explosions, using both whitened and unwhitened data, shows that spectral nulls are enhanced in the whitened spectra. Network summed spectra (unwhitened) for seventeen earthquakes are also included; these demonstrate the fact that nulls can be caused, for example, by multipath effects and multiplet sources as well as by depth-phase interference.

TABLE OF CONTENTS

LIST OF FIGURES

LIST OF FIGURES (Cont'd.)

LIST OF FIGURES (Cont'd.)

LIST OF TABLES

INTRODUCTION

The objective of this work is to demonstrate a method for whitening teleseismic spectra. As applied to explosion data, the method can enhance spectral characteristics associated with interference of the type pP-P, and thus aid in source depth analysis. Previous depth-determination analyses (Cohen, 1970) have employed individual station spectra, which in an attempt to enhance spectral components in the band 2 to 5 Hz were corrected for instrument response. Further, to reduce reverberation noise at the individual recording sites, analysis was performed on a network-averaged spectrum. Despite this processing, the network-summed spectra were still band-limited (primarily by the earth's transmission characteristics), and generally exhibited a single spectral null which could be interpreted as deriving from depth-phase interference.

To enhance spectral characteristics in the band 2-5 Hz, teleseismic spectra require whitening. Here we whiten the spectra by dividing out a path-recording site response which is determined by averaging spectra from a suite of events as determined from data recorded at a single station. The whitened spectra from a single event are then summed over the recording network to yield the average spectra u ed in depth-phase analysis.

While the proposed analysis technique can enhance spectral characteristics, we must add that scalloped spectra can be caused by multi-path effects and multiplet sources as well as by depth-phase interference.

Examples of scalloped earthquake spectra are shown in the Appendix. Thus, caution must be exercised in using spectral-null depth determinations as a diagnostic.

METHOD

Let

$E_i(f)$ = source spectrum

$S_i(f)$ = explosion site crustal response

$P_{ij}(f)$ = mantle path response

$R_j(f)$ = receiving site crustal response

$I_j(f)$ = instrument response

Then, for the i'th underground shot as recorded at the j'th station, the observed short-period spectrum $\phi_{ij}(f)$ is given by:

$$\phi_{ij}(f) = E_i(f) \cdot S_i(f) \cdot P_{ij}(f) \cdot R_j(f) \cdot I_j(f) \cdot [1 + \alpha^2 + 2\alpha\cos(\omega\tau_{ij})], \quad (1)$$

where the quantity in square brackets is the pP-P interference function, α is the free-surface reflection coefficient, and τ_{ij} is the depth-phase delay time at the j'th station for the i'th shot. Note that:

$\tau_{ij} \simeq \tau_{im}$, and can be taken simply as τ_i;

however,

$\tau_{ij} \neq \tau_{mj}$,

since in this work we will use a suite of shots having

various source depths. In previous work Cohen (1970) used a network-average spectrum to enhance pP-P spectral periodicities. Further, the individual station spectra were corrected for instrument response. The network-average spectrum used for depth-determination analysis, therefore, is given by:

$$\overline{\Phi}_i(f) = \frac{1}{N} E_i(f) \cdot S_i(f) \{\sum_j [P_{ij}(f) \cdot R_j(f)]\} \cdot [1 + \alpha^2 + 2\cos(\omega\tau_i)] \quad (2)$$

where the sum is performed over the spectra at N recording sites. Implicit in the above relation is the assumption that 'holes' in the spectra which are caused by the geology at the individual recording sites and along the source-receiver paths will in large part average out. If this assumption holds, and both $E_i(f)$ and $S_i(f)$ change slowly over the band 0.3-5 Hz, the character of $\phi_i(f)$ will be controlled by the cosinusoidal depth-phase function. That is:

$$\overline{\Phi}_i(f) \approx E_i(f) \cdot S_i(f) \cdot [1 + \alpha^2 + 2\alpha\cos(\omega\tau_i)] \cdot \overline{PR}, \quad (3)$$

where

$$\overline{PR} \equiv \frac{1}{N} \sum_j P_{ij}(f) \cdot R_j(f).$$

Though application of this technique has met with some success (Lambert et al., 1969; Cohen, 1970), the method is not without its shortcomings. While we may be reasonably assured that $E_i(f)$ varies slowly in the

frequency band of interest (cf. Wyss et al., 1971), Wirth (1971) has shown that for interval reflection coefficients somewhat more extreme than are usually found, teleseismic spectra can be considerably complicated due to the effects of $S_i(f)$. Further, the effect of $P_{ij}(f)$ for every shot-station pair is approximately the same, generally to attenuate the higher frequencies; the result is that short-period spectra are severely band-limited. Finally, from a practical point of view, a large number of recording stations -- say 10 -- is not always available for network averaging, and so the $\overline{\phi}_i(f)$ may still reflect contributions from the $R_j(f)$. In sum, the network-averaged spectrum $\overline{\phi}_i(f)$ tends to be complicated, showing predominance of energy in the 0.5 - 2.0 Hz band, and often exhibits only a single spectral null which can be attributed to interference between P and pP. Two examples supporting the above observations are given in Figures 1a and 1b. In the case of GASBUGGY, the P_n spectra for 12 stations were averaged; for LONG SHOT, 31 station spectra were used. In both cases the network-averaged spectra are band-limited and exhibit a single broad spectral null which has been interpreted as the depth-phase null.

Suppose now that we have a network consisting of several seismic stations, each of which records the signals from a group of explosions in the same general epicentral region. Further, let the explosions be at various depths. Summing over spectra <u>at a single station</u>, we have:

$$\overline{\phi}_j(f) = \frac{1}{M} \{\sum_i E_i(f) \cdot S_i(f) \cdot P_{ij}(f) \cdot [1 + \alpha^2 + 2\alpha \cos(\omega\tau_{ij})]\} \cdot R_j(f) \qquad (4)$$

when the sum is performed over M explosions.
But

$$\bar{\phi}_j(f) \approx \frac{1}{M} E(f) \cdot P_j(f) \cdot R_j(f) \{\sum_i S_i(f)[1 + \alpha^2 + 2\alpha\cos(\omega\tau_{ij})]\} \quad (5)$$

since in the frequency band of interest, $E_i(f) \approx E_m(f) = E(f)$, and the path from the explosions to a given receiver are virtually identical (i.e., $P_{ij}(f) \approx P_{mj}(f) = P_j(f)$). With the exception of spectral characteristics due to gross crustal structures at the source, we would expect the factor

$$\frac{1}{M} \sum_i S_i(f) \cdot [1 + \alpha^2 + 2\alpha\cos(\omega\tau_{ij})] \equiv \overline{SD} \quad (6)$$

to be a smoothly varying function.
Thus

$$\bar{\phi}_j(f) = E(f) \cdot P_j(f) \cdot R_j(f) \cdot \overline{SD} \quad (7)$$

Let us now use the $\bar{\phi}_j(f)$ to correct the raw observed spectra. Again, instrument response has been removed, although it would have canceled anyway in the case of identically equipped stations. Thus:

$$\theta_{ij}(f) = \frac{\phi_{ij}(f)}{\bar{\phi}_j(f)} = \frac{E(f) \cdot S_i(f) \cdot P_j(f) \cdot R_j(f) \cdot [1 + \alpha^2 + 2\alpha\cos(\omega\tau_{ij})]}{E(f) \cdot P_j(f) \cdot R_j(f) \cdot \overline{SD}} \quad (8)$$

$$= \frac{1}{\overline{SD}} S_i(f) \, [1 + \alpha^2 + 2\alpha\cos(\omega\tau_{ij})]$$

Averaging the $\theta_{ij}(f)$ over the network of recording stations yields

$$\overline{\theta}_i(f) = \frac{1}{N \cdot \overline{SD}} S_i(f) \cdot \sum_j [1 + \alpha^2 + 2\alpha\cos(\omega\tau_{ij})]$$
$$\simeq \frac{S_i(f)}{\overline{SD}} \cdot [1 + \alpha^2 + 2\alpha\cos(\omega\tau_i)], \qquad (9)$$

where $(S_i(f)/\overline{SD})$ should now contain only the more minor contributions from S_i, that is, the contributions due to small-scale layered structures particular to a given explosion site.

Comparing equation (9) with equation (3), we see that the proposed analysis method, through the removal of source and path responses, may be expected to yield a whitened network-average spectrum, enriched, for example, in the scalloped components produced by pP-P interference.

TEST OF THE PROPOSED METHOD

We first test the proposed analysis method on simulated teleseismic data. Specifically, we will generate short-period seismograms at seven hypothetical receiving stations for seven hypothetical underground explosions. The receiving stations are assumed to have a world-wide distribution, and so, the crustal sections from station to station can exhibit large-scale differences. On the other hand, the explosions are assumed detonated in a region of small dimensional extent and as such, only very minor changes in velocities and layer thickness are permitted from site to site.

The model used to simulate a nuclear explosion has a power spectrum given by Haskell (1967). Using this model, a minimum phase signal for a 100 kT explosion in granite was computed. This signal was then filtered to incorporate the short-period Benioff response (pendulum and glavonmeter damping taken as 1.0; pendulum free period: 1.25 sec; galvonometer free period: 0.2 sec). The resulting wavelet, which was convolved with the spike seismograms corresponding to the various crustal models employed, is shown in Figure 2. A Monte Carlo technique was used to generate layer models for both the source and receiver sites. Basic to each crustal model was the realistic gross velocity-depth distribution shown in Figure 3. Random variations to this model were introduced to produce the crustal structures at the source and receiver sites (Figures 4, and 5 through 8, respectively). Because the explosions

were assumed detonated in the same general area, only minor variations in the velocities and layer thickness of a single gross crustal model were permitted from one source site to another. As such, the crustal models for the shot sites are virtually identical to that shown in Figure 4. On the other hand, the crustal models for the seven receiver sites display marked differences; this is expected for sites located in widely separated geological provinces.

Given the layered models, synthetic seismograms were computed which took into account all reflections occurring at interfaces to approximately 200 km depth at both the source and receiver. An efficient solution for the combined source and receiver stack given by Wirth (1971) was used to generate the synthetic seismograms. The program generates solutions for a specified number of receivers in fixed positions for a specified number of explosion sources of given depths. Depths for the hypothetical events used here are listed in Table I, together with the frequency of the first spectral null for a nominal overburden velocity of 3 km/sec. The synthetic seismograms so generated are shown in Figures 9 through 15.

Application of the depth-analysis technique described by Cohen (1970) and that proposed here yields the results shown in Figures 16 through 19. Spectra have been smoothed with a 15-point running average to enhance the display of broad nulls which might be associated with pP. Frequencies where nulling is observed are summarized in Table II, together with implied source

depths based on a nominal over-burden velocity of 3 km/sec. Actually, average overburden velocities for the hypothetical shots varied from 3.1 to 3.5 km/sec, depending on the shot depth. As such, depth estimates in Tables I and II are somewhat shallow.

As seen from Table II, the depth-phase analysis method employing unwhitened data yielded results in only three cases; in each of these cases, the depth of the event is greater than 1.0 km. The proposed depth analysis method, however, yielded satisfactory results in every case, with shot depths ranging from 0.7 to 1.4 km. It must be admitted, however, that a plot of the unwhitened spectra on a log scale would also show at least a significant first null in every case. We see that defining the word "significant" is difficult.

RESULTS - EXPERIMENTAL

Application of the proposed analysis method to real data presents some problems. In the previous theoretical example, every station "recorded" signals from every shot; we find for real data that the more stations we consider, the fewer common shots we have available (and vice versa). This, of course, is a consequence of not having some given set of LRSM and observatory stations continuously operative. Nonetheless, it is still possible to test the method using the data recorded at seven stations for three to seven NTS events. Station locations relative to NTS are given in Figure 20, while pertinent shot data is listed in Table III. Table IV lists the shot data used for each station.

Inspection of Table III shows that four of the seven shots to be used have depths in the range .55 to .67 km. Thus, we considered the possibility of weighting the spectra for these four shots such that the spectral sum over the suite of events at any given station would not be biased by the characteristics of shots in this depth range. That is, we were somewhat apprehensive about the effectiveness with which the cosinusoidal depth phase functions would average out (equation (6)) for the shots considered. On the other hand, in a real analysis situation, we would not know the event depths a priori. As such, we decided to weight the shot spectra equally.

Average station spectra obtained by summing over

the available shot spectra at a given station are shown in Figure 21. Except for the average spectra at CPO and KC-MO, the average station spectra show a single, broad spectral rise with peak power observed in the band .7 - .9 Hz. The spectra at three stations -- HN-ME, RK-ON, and SV3QB -- exhibit slight nulling between .9 - 1.0 Hz, but these nulls are considered second-order characteristics. Presumably then, the average station spectra $\overline{\phi}_j(f)$ at HN-ME, PG-BC, RK-ON, SV3QB, and WMO primarily exhibit the product of path and recording site crustal responses for each station (equation (7)).

The average station spectra at CPO and KC-MO are somewhat more complicated than the spectra at other stations. Whether we are seeing real perturbations caused by path and site responses, or merely the results of averaging over an insufficient number of shots (CPO:3; KC-MO:5) is a matter of conjecture. Because of the shot-depth distributions for events recorded at CPO and KC-MO (Table III), we would expect the average station spectra at these stations to exhibit some nulling effects due to shots with depths between 0.55 and 0.67 km. However, we will proceed with the analysis using all of the spectra shown in Figure 21, again emphasizing our blindness to shot depth distribution.

Spectral null analyses performed on the raw spectra and on those spectra corrected for path and site response, are shown in Figures 22 through 35. The results are presented in pairs, grouped by shot. The bottom trace in each case is the average network

spectrum computed over the suite of individual station spectra.

BOXCAR (Figures 22 and 23)

A conventional null-frequency analysis (Cohen, 1970) performed using spectra at five LRSM stations is shown in Figure 22. All station spectra show a sharp drop in power at .9 Hz, with nulls clearly visible near this frequency in the spectra at HN-ME and SV3QB. A sum over the station network exhibits a null at .93 Hz. Provisionally interpreting this null to derive from pP-P interference, and taking .93 Hz as the null-frequency increment, the corresponding depth-phase delay time is 1.07 seconds.

Analysis of the station spectra corrected for path and site response (Figure 23) lends credence to the above result. All station spectra now exhibit a null near .9 - 1.0 Hz. Further, several spectra show a second drop in power near 1.8 Hz, with a null at this frequency observed in the SV3QB spectrum. The network-summed spectrum exhibits a null at 0.95 and a weak null at 1.80 Hz, suggesting a null-frequency increment of 0.9 Hz. This yields an estimated depth-phase delay time for the event of 1.1 seconds.

CHARTREUSE (Figures 24 and 25)

Conventional depth-phase analysis using the spectra at six stations is shown in Figure 24. All spectra show a significant drop in power near 1.3 - 1.4 Hz,

with nulls observed near these frequencies at KC-MO, PG-BC, and SV3QB. The network sum shows a slight depression at about 1.45 Hz. Taking 1.45 Hz as the null-frequency increment for interference of the type pP-P yields a depth-phase delay time of .69 second.

Results obtained using corrected station spectra (Figure 25) are somewhat ambiguous. While broad nulls are observed in the average spectrum at 1.4 and 2.6 Hz, one might argue that these nulls are the second and fourth in a series have a null-frequency increment of .6 to .7 Hz. However, nulls at 0.6 and 1.9 Hz are poorly developed. These data then, suggest a null-frequency increment of 1.3 Hz, with a corresponding depth-phase delay time of .77 second.

DURYEA (Figures 26 and 27)

Conventional spectra-null analysis yields the results shown in Figure 26. A broad null near 1.7 Hz is observed in the network-summed spectrum, though this feature is not well developed. As such, the data suggest a null-frequency interval of 1.7 Hz, with a corresponding delay time of .59 second.

Null-frequency analysis for DURYEA using spectra corrected for path and site response (Figure 27) yields a similar result. Again, a null in the average spectrum is observed near 1.7 Hz, with another poorly developed, broad null around 3.25 Hz. Nulls at 1.7 Hz are observed in the spectra for CPO, HN-ME and SV3QB with the spectrum at the latter station also exhibiting a null

at 3.4 Hz. For this shot, then, nulls provisionally interpreted as due to pP-P interference are observed with possible null-frequency increments of 1.7 Hz, yielding a corresponding estimate for the depth-phase delay time of 0.59 second.

GREELEY (Figures 28 and 29)

Inspection of the spectra obtained through conventional null-frequency analysis (Figure 28) shows several stations to exhibit nulls near 1 Hz. The null at 1 Hz observed at SV3QB is particularly well developed. Upon summing over station spectra, however, we obtain an average spectrum devoid of nulls. As such, spectral-null analysis using the unprocessed station spectra is not recommended.

Recourse to the processed station spectra (Figure 29) yields a most satisfactory result. A spectral null in the vicinity of 1 Hz is observed at every station, with the spectra at HN-ME and PG-BC also exhibiting weak nulls near 2 Hz. We are therefore inclined to adopt a null-frequency interval of 1 Hz, with a corresponding depth-phase delay time of one second.

HALF-BEAK (Figures 30 and 31)

Conventional depth-phase analysis for HALF-BEAK (Figure 30) yields a questionable result. Spectra at KC-MO and RK-ON exhibit weak nulls around 1.2 Hz, with a very weak null observed in the network-averaged spectrum at 1.25 Hz. Though speculative, we

adopt 1.25 Hz as the null-frequency interval, yielding a depth-phase delay time of 0.80 second.

Using spectra corrected for path and site response (Figure 31) yields a somewhat more reliable estimate of the null-frequency interval. Here, a null in the network-averaged spectrum is clearly observed at 1.15 Hz, with a weak null present around 2.0 Hz. Taking 1.15 Hz, as the average null-frequency interval, we compute a depth-phase delay time of 0.87 second.

KNICKERBOCKER (Figures 32 and 33)

Conventional depth-phase analysis (Figure 32) suggests the presence of a broad null centered at 1.4 Hz, perhaps best developed in the spectrum for HN-ME. As such, the null-frequency interval will be taken as 1.4 Hz, yielding a depth-phase delay time of 0.7 second.

Employing the proposed spectral whitening technique yields an interesting result (Figure 33). Nulls in the network-averaged spectrum are observed at 1.30 and 2.15 Hz with nulls at these frequencies best developed in the station spectra for CPO, HN-ME, PG-BC and WMO. Further, the CPO spectrum also exhibits nulls at 0.40 and 2.85 Hz. This suggests that the null frequencies are given by the formula:

$$f_n = (2n+1)f_o, \qquad n = 0,1,2,\ldots,$$

where $f_o \approx 0.42$ Hz. But this implies that the null phenomenon observed here is caused by the interference of two similar signals arriving with the same first-motion

polarity, with the second signal delayed $1/(2f_o)$ or 1.2 seconds relative to the first signal. The second signal presumably is produced by spalling of the near-surface layers (Eisler and Chilton, 1964), and will therefore be referred to as P_{SPALL}.

In the case of KNICKERBOCKER, then, spectral nulling is apparently controlled by interference of the type P_{SPALL}-P, with interference of the type pP-P less well developed, if developed at all. As such, the depth estimate previously obtained using the unwhitened KNICKERBOCKER data is suspect, for the null at 1.4 Hz observed in the network-averaged spectrum (Figure 32) is probably related to P_{SPALL}-P interference.

REX (Figures 34 and 35)

The network-average spectrum obtained using conventional analysis techniques (Figure 34) yields an ambiguous result. A well-developed null is observed at 1.4 Hz, and taking this frequency as the null frequency interval yields a depth-phase delay time of 0.7 second. On the other hand, a weak null in the average spectrum is observed at 2.3 Hz, with the suggestion of a null also seen at 0.45 Hz. These nulls, together with the null at 1.4 Hz, suggest a null frequency interval of 0.9 Hz, with nulling presumably due to P_{SPALL}-P interference. If the latter explanation is correct, P_{SPALL} arrives 1.1 seconds after the P arrival.

Application of the spectral whitening technique yields a negative result. Numerous nulls are observed in the individual station spectra, but little

consistency in the null frequencies is observed from station to station. As such, it is not surprising to find that the network-averaged spectrum displays little character. The spectra for several stations (PG-BC, RK-ON, and SV3QB) do exhibit broad peaks centered near 3.3 Hz, with addendant nulling suggested in the band 1.7-2 Hz. Whether this broad nulling is due to pP-P or P_{SPALL}-P interference, however, is purely speculative.

DISCUSSION

Depth-phase analysis resuls are shown in Figure 36. Results for KNICKERBOCKER and REX are not included. To facilitate a determination of average overburden velocity, the delay times are plotted against double the known shot depths.

Both the whitened and unwhitened spectra yield a consistent set of delay-time determinations. In general, nulls in the spectra corrected for site and path response are more enhanced than those observed in spectra not corrected for these effects. The data suggest an average overburden velocity of 1.8 km/sec to depths on the order of 0.6 km, with an increase to 3 km/sec suggested at greater depths. This results in good agreement with the upper crustal model for the Yucca Flat area of NTS given by Glover and Alexander (1970). Their model shows a surface layer 0.2 km thick with a compressional velocity of 1.3 km/sec followed by a layer 0.8 km thick with a velocity of 3.0 km/sec.

CONCLUSIONS

1. Teleseismic spectra can be whitened by dividing out a path-recording site response determined by averaging spectra from a suite of events as determined from the data at a single station. Source spectral characteristics can then be enhanced by averaging the individual whitened spectra over the recording network. Implicit in this type of analysis is the requirement that a network of common stations has recorded signals from a suite of events.

2. The whitening process tends to enhance spectral components in the band 2 - 5 Hz. As such, the method may be useful in the analysis of spectral characteristics (nulls) provisionally interpreted as due to pP-P interference.

3. Analysis of short-period data for seven NTS explosions shows that the sought-after depth-phase spectral nulls can be enhanced through application of the proposed spectral whitening technique. The whitened spectra, however, are somewhat more complicated than the unwhitened spectra, and accordingly, are more difficult to interpret.

4. Recognizing that both pP-P and P_{SPALL}-P interference can be present in teleseismic P spectra suggests that more objective techniques for examining spectral characteristics (e.g., the pseudo-autocorrelation and the cepstrum) be employed in null-frequency analysis.

REFERENCES

Cohen, T.J., 1970, Source-depth determinations using spectral, pseudo-autocorrelation and cepstral analysis: Geophys. J.R. Astr. Soc., v. 20, p. 223-251.

Eisler, J.D. and Chilton, F., 1964, Spalling of the earth's surface by underground nuclear explosions: Jour. Geophys. Res., v. 69, No. 24, p. 5285-5293.

Evernden, J.A., 1970, Magnitude versus yield of explosion: Jour. Geophys. Res., v. 75, No. 5, p. 1028, 1032.

Glover, P. and Alexander, S.S., 1970, A comparison of the Lake Superior and Nevada Test Site source regions: Seismic Data Laboratory Report No. 243, Teledyne Geotech.

Haskell, N.A., 1967, Analytic approximation for the elastic radiation from a contained underground explosion: Jour. Geophys. Res., v. 72, No. 10, p. 2583-2587.

Lambert, D.G., von Seggern, D.H., Alexander, S.S., and Galat, G.A., 1969, The LONG SHOT experiment - Vol. II - Comprehensive analysis: Seismic Data Laboratory Report No. 234, Teledyne Geotech, Alexandria, Virginia.

Wirth, M.H., 1971 (pending), Time and frequency domain solutions for vertically-incident waves in multi-layered absorptive media with application to source-depth determination: Seismic Data Laboratory Report, Teledyne Geotech, Alexandria, Virginia.

Wyss, M., Hanks, C. and Liebermann, R.C., 1971, Comparison of P-wave spectra of underground explosions and earthquakes: Jour. Geophys. Res., v. 76, No. 11, p. 2716-2729.

ACKNOWLEDGEMENT

We are grateful to D.H. von Seggern for his comments on spalling, and for his critical reading of the manuscript.

TABLE I

Shots Depths and Nominal First-Null Frequencies

SHOT	DEPTH	f_1^*
1	.708	2.12
2	1.349	1.11
3	.772	1.94
4	.883	1.70
5	1.169	1.28
6	.695	2.16
7	1.101	1.36

*Overburden velocity of 3.0 km/sec assumed

TABLE II

Observed Null Frequencies and Implied Depths

SHOT and METHOD*	f_1	f_2	f_3	$\bar{f}$	IMPLIED DEPTH (km) $\bar{V}$ = 3 km/sec	KNOWN DEPTH (km) (INPUT)
1-A	--	--	--	--	--	0.71
1-B	2.50	4.70	--	2.35	0.64	0.71
2-A	1.25	--	--	1.25	1.20	1.35
2-B	1.20	2.45	3.85	1.28	1.17	1.35
3-A	--	--	--	--	--	0.77
3-B	1.95	3.95	--	1.98	0.76	0.77
4-A	--	--	--	--	--	0.88
4-B	1.85	3.80	--	1.90	0.79	0.88
5-A	1.45	--	--	1.45	1.04	1.17
5-B	1.40	3.00	4.20	1.40	1.07	1.17
6-A	--	--	--	--	--	0.70
6-B	2.40	(5.00)	--	2.40	0.62	0.70
7-A	1.45	--	--	1.45	1.04	1.10
7-B	1.40	2.95	4.15	1.38	1.09	1.10

*A - Cohen (1970)

B - Present Paper

TABLE III

NTS Event Descriptions

EVENT	DATE	TIME (Z)	m_b	LATITUDE (°N)	LONGITUDE (°W)	GEOLOGIC MEDIUM	SHOT DEPTH (ft)	(km)
BOXCAR	26 Apr 68	15:00:00.0	6.4	37°17'44.0"	116°27'21.0	Rhyolite	3800	1.158
CHARTREUSE	06 May 66	15:00:00.1	5.2	37°20'53.0"	116°19'19.0"	Rhyolite	2195	.669
DURYEA	14 Apr 66	14:13:43.1	5.2	37°14'34.0"	116°25'51.0"	Rhyolite	1795	.547
GREELEY	20 Dec 66	15:30:00.1	6.3	37°18'07.0"	116°24'30.0"	Zeolitized Tuff	4040	1.231
HALF BEAK	30 Jun 66	22:15:00.1	6.0	37°18'57.0"	116°17'56.0"	Rhyolite	2884	.879
KNICKERBOCKER	26 May 67	15:00:00.0	5.5	37°14'53.0"	116°28'49.0"	Rhyolite	2080	.634
REX	24 Feb 66	15:55:07.0	4.8	37°16'19.0"	116°26'02.0"	Tuff	2200	.671

TABLE IV

RECORD OF SEISMOGRAM AVAILABILITY

EVENT	STATION CPO	HN-ME	KC-MO	PG-BC	RK-ON	SV3QB	WMO	TOTAL STATIONS
BOXCAR		*		*	*	*	*	5
CHARTREUSE		*	*	*	*	*	*	6
DURYEA	*	*	*	*	*	*	*	7
GREELEY		*	*	*	*	*	*	6
HALF BEAK		*	*	*	*	*	*	6
KNICKERBOCKER	*	*		*	*	*	*	6
REX	*		*	*	*	*	*	6
TOTAL SHOTS	3	6	5	7	7	7	7	

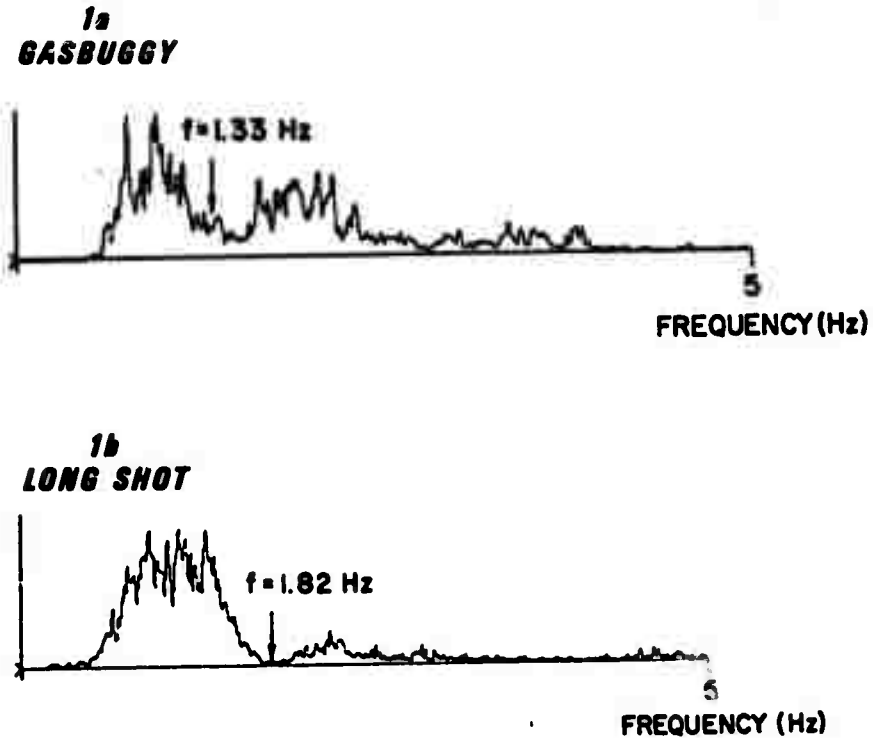

Figure 1. Spectral null analysis a) GASBUGGY b) LONG SHOT.

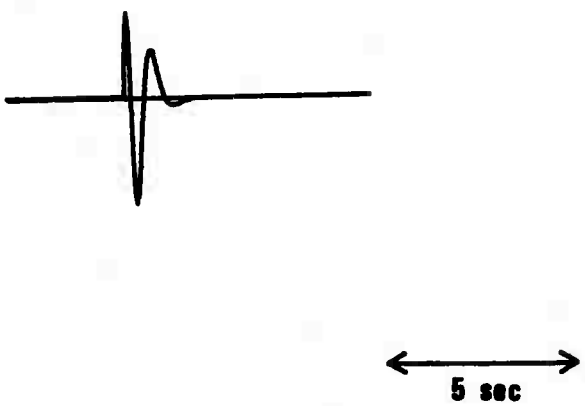

Figure 2. Minimum-phase wavelet.

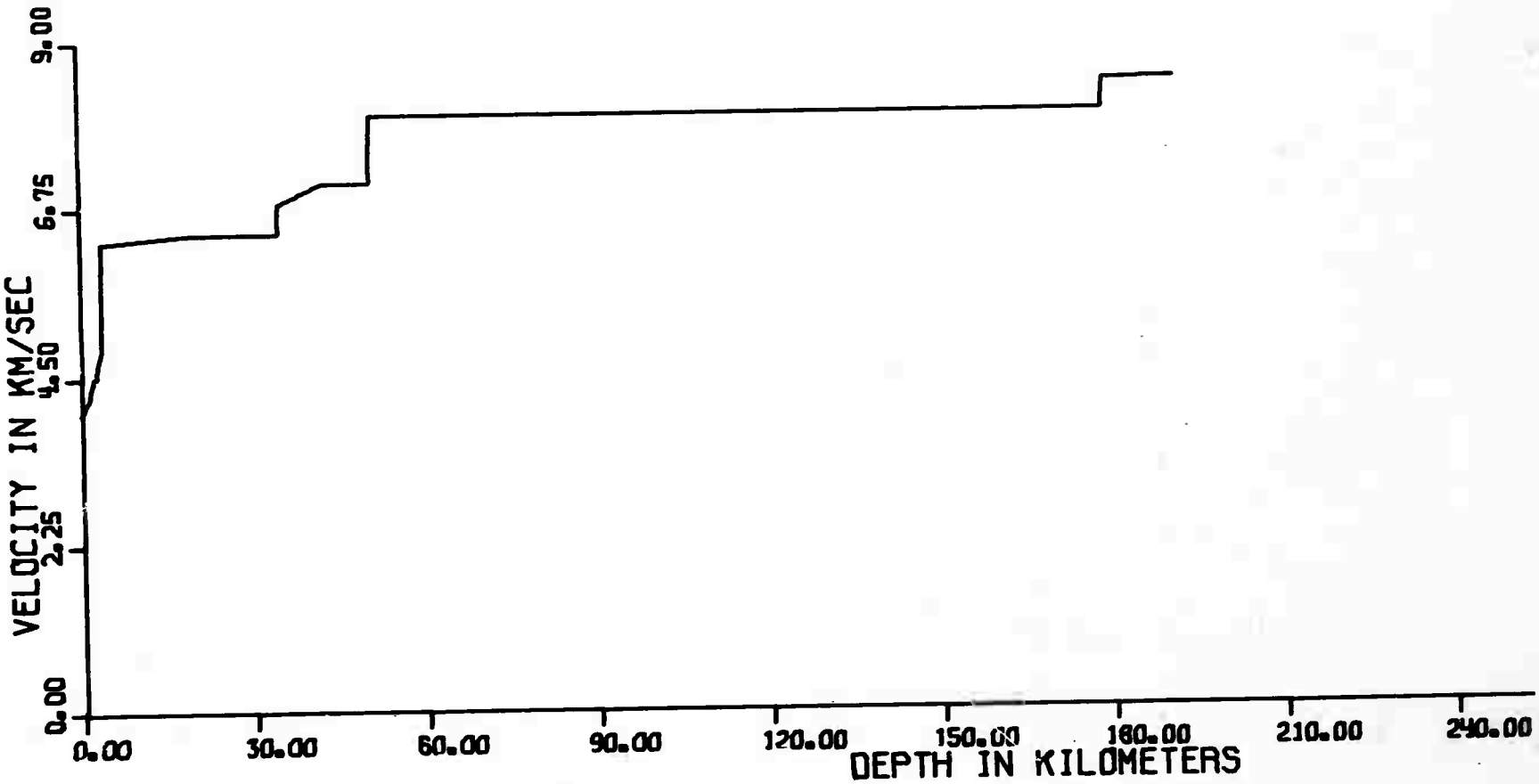

Figure 3. Gross crustal model from which source and receiver models are derived by the Monte Carlo technique.

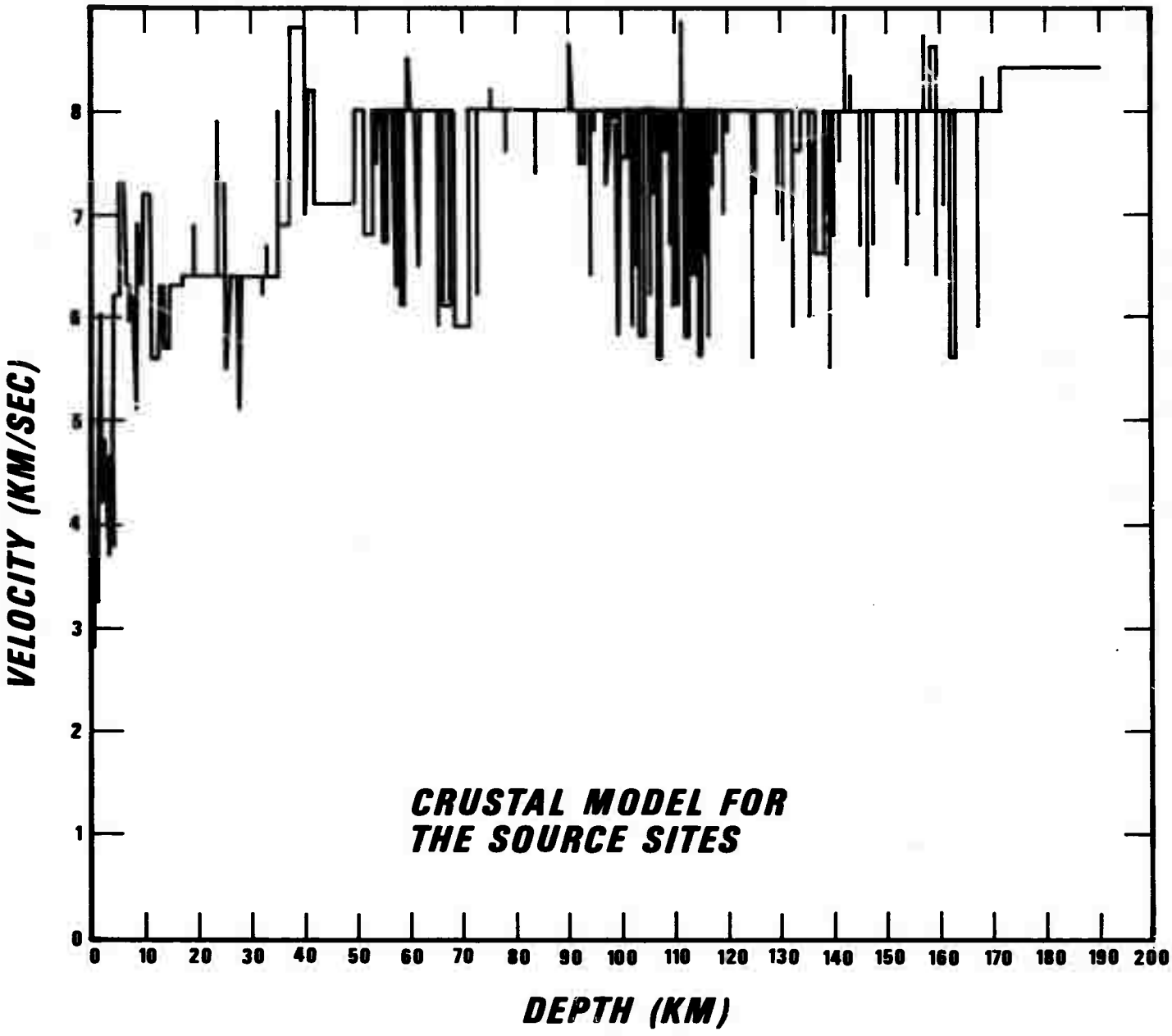

Figure 4. Crustal model for the source sites.

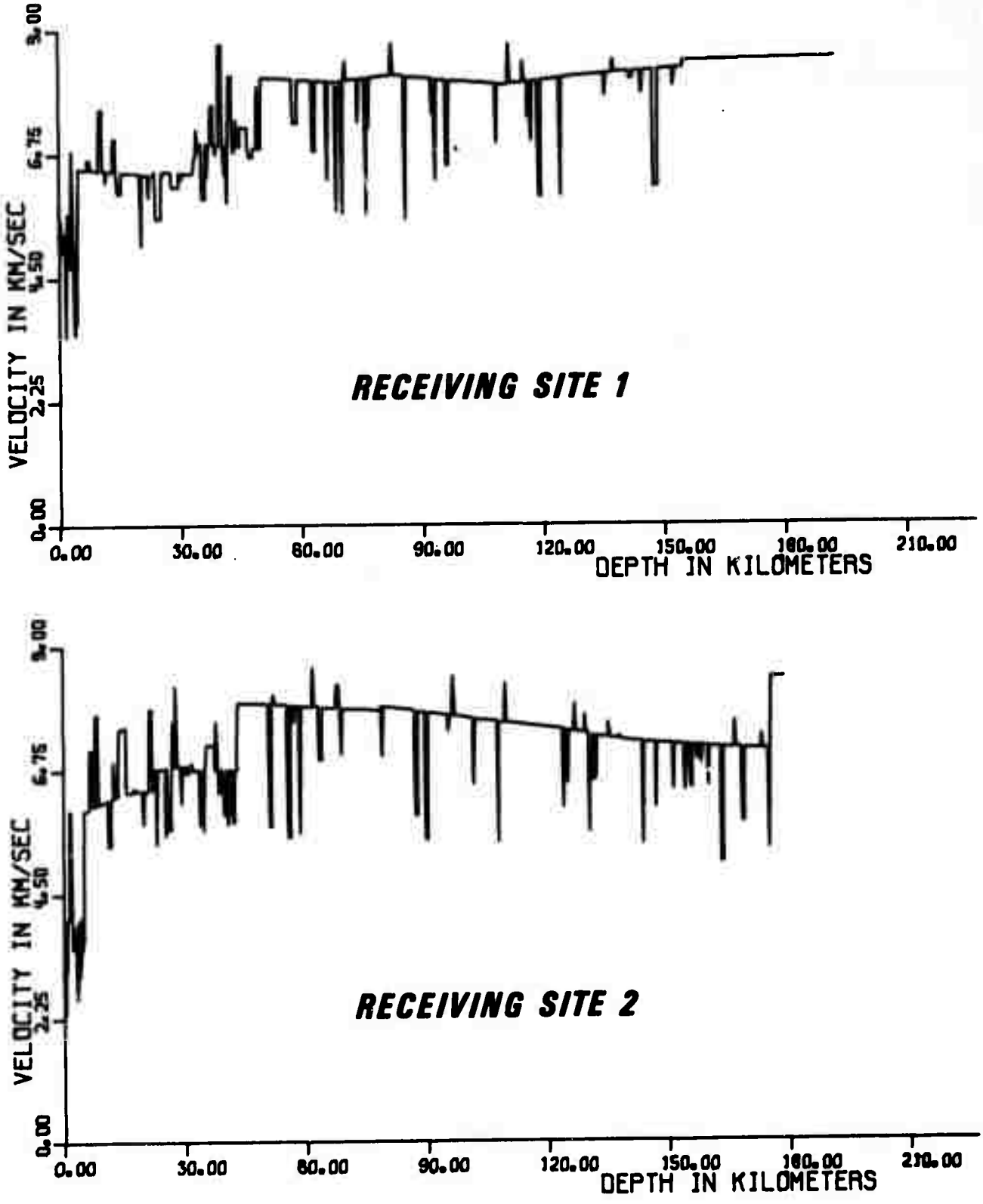

Figure 5. Crustal models for receiving sites 1 and 2.

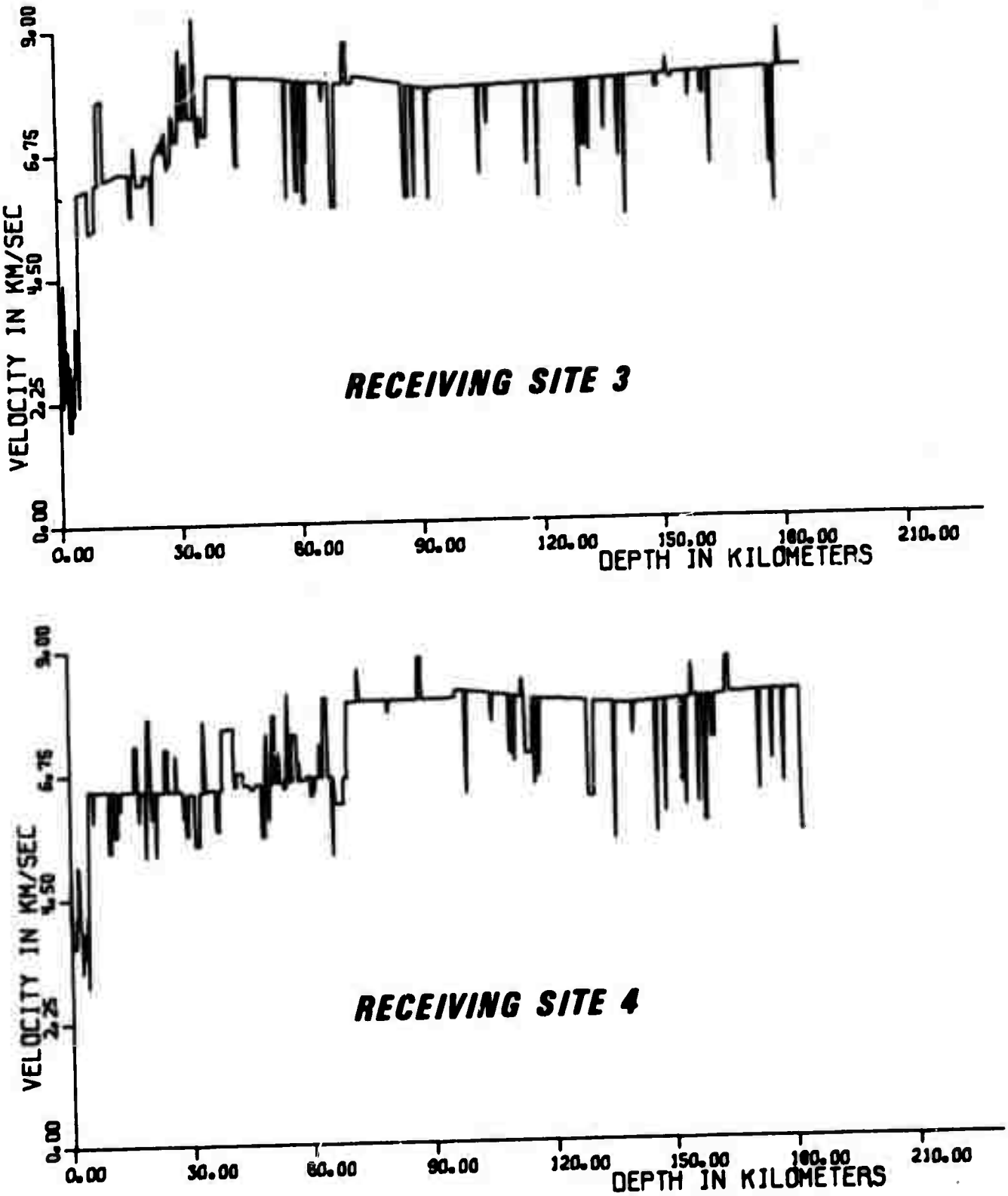

Figure 6. Crustal models for receiving sites 3 and 4.

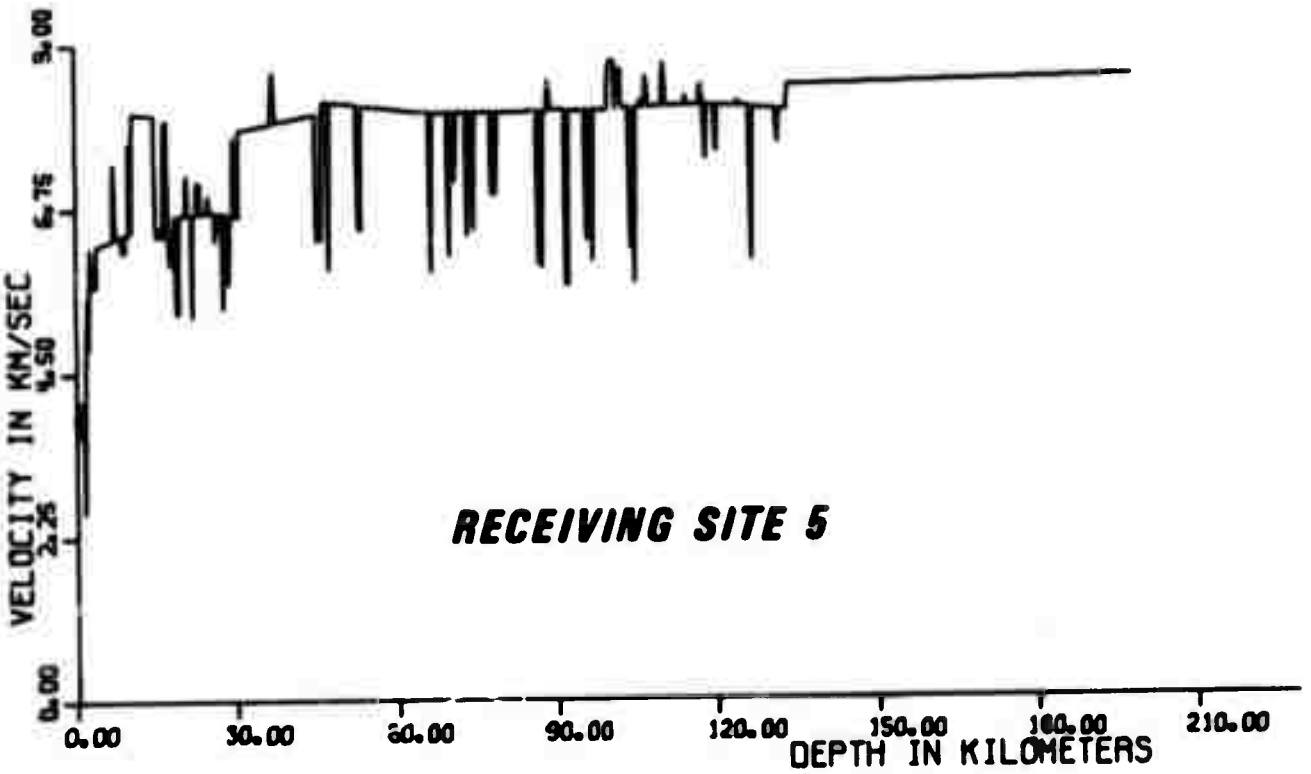

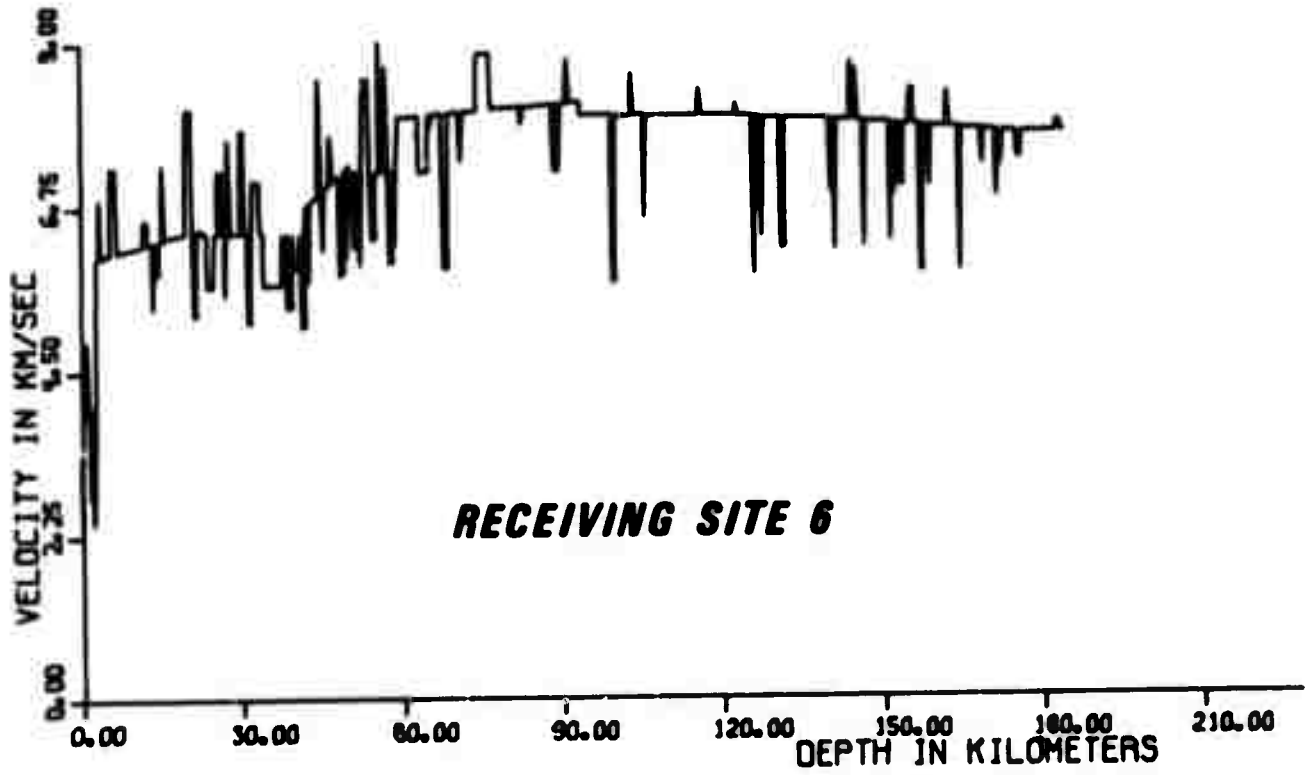

Figure 7. Crustal models for receiving sites 5 and 6.

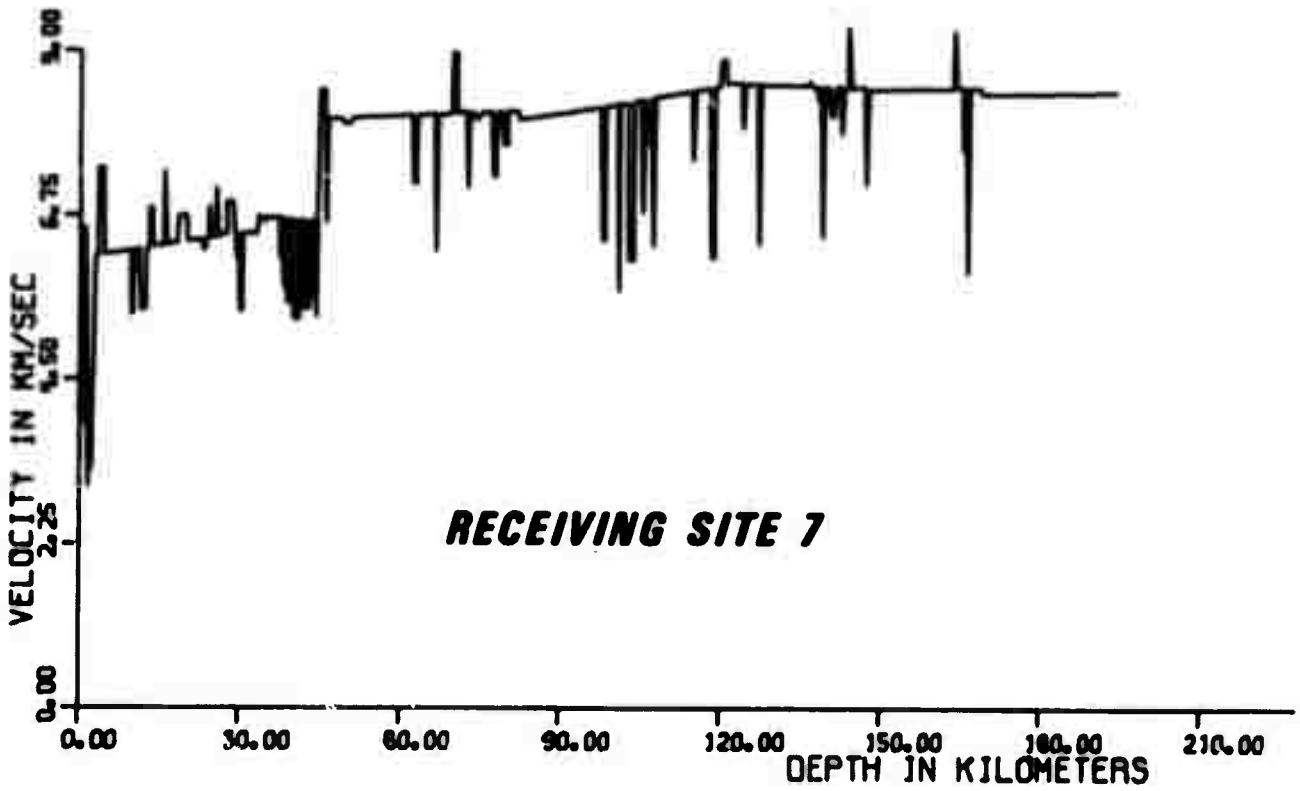

Figure 8. Crustal model for receiving site 7.

Figure 9. Theoretical station seismograms, Shot 1.

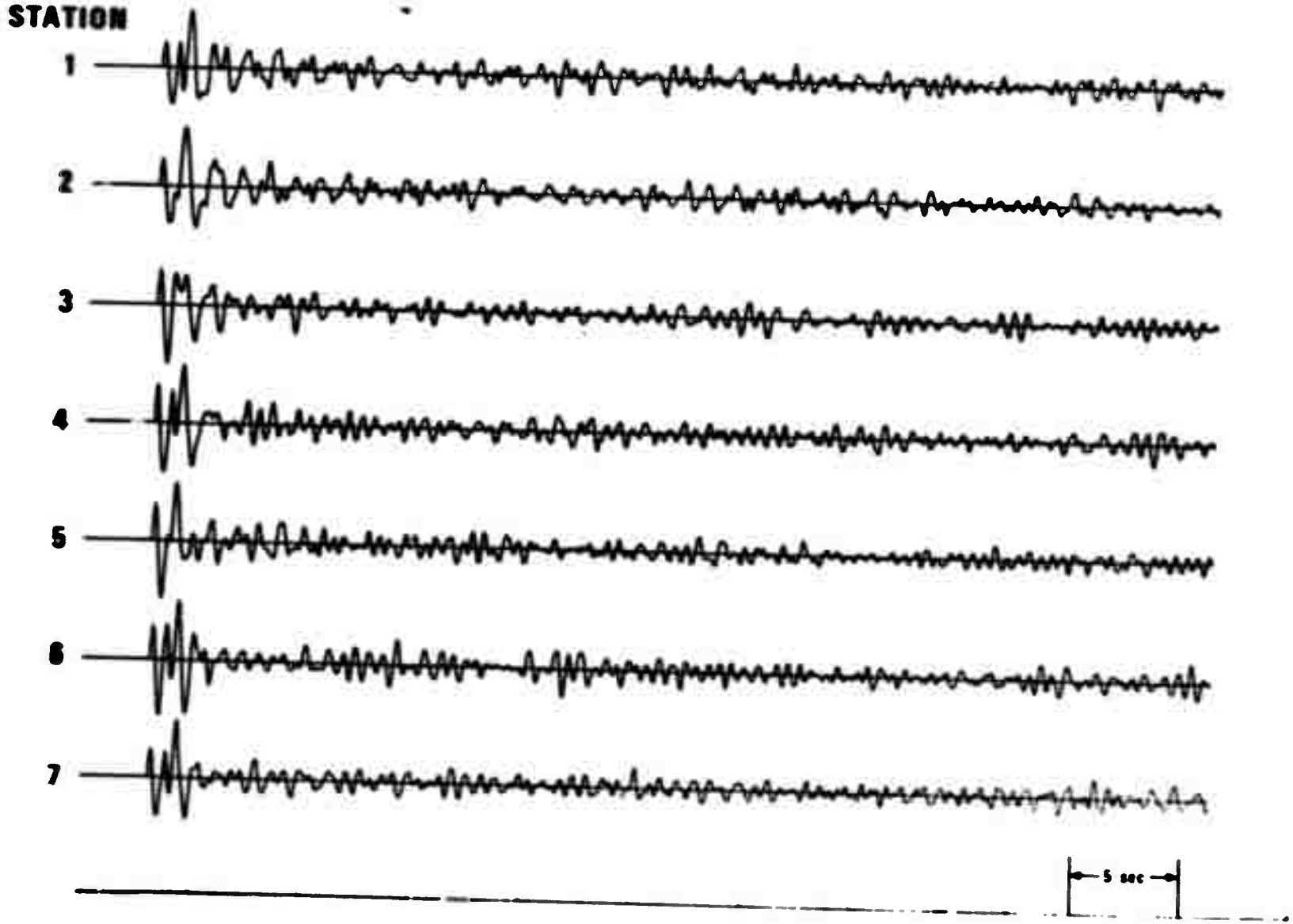

Figure 10. Theoretical station seismograms, Shot 2.

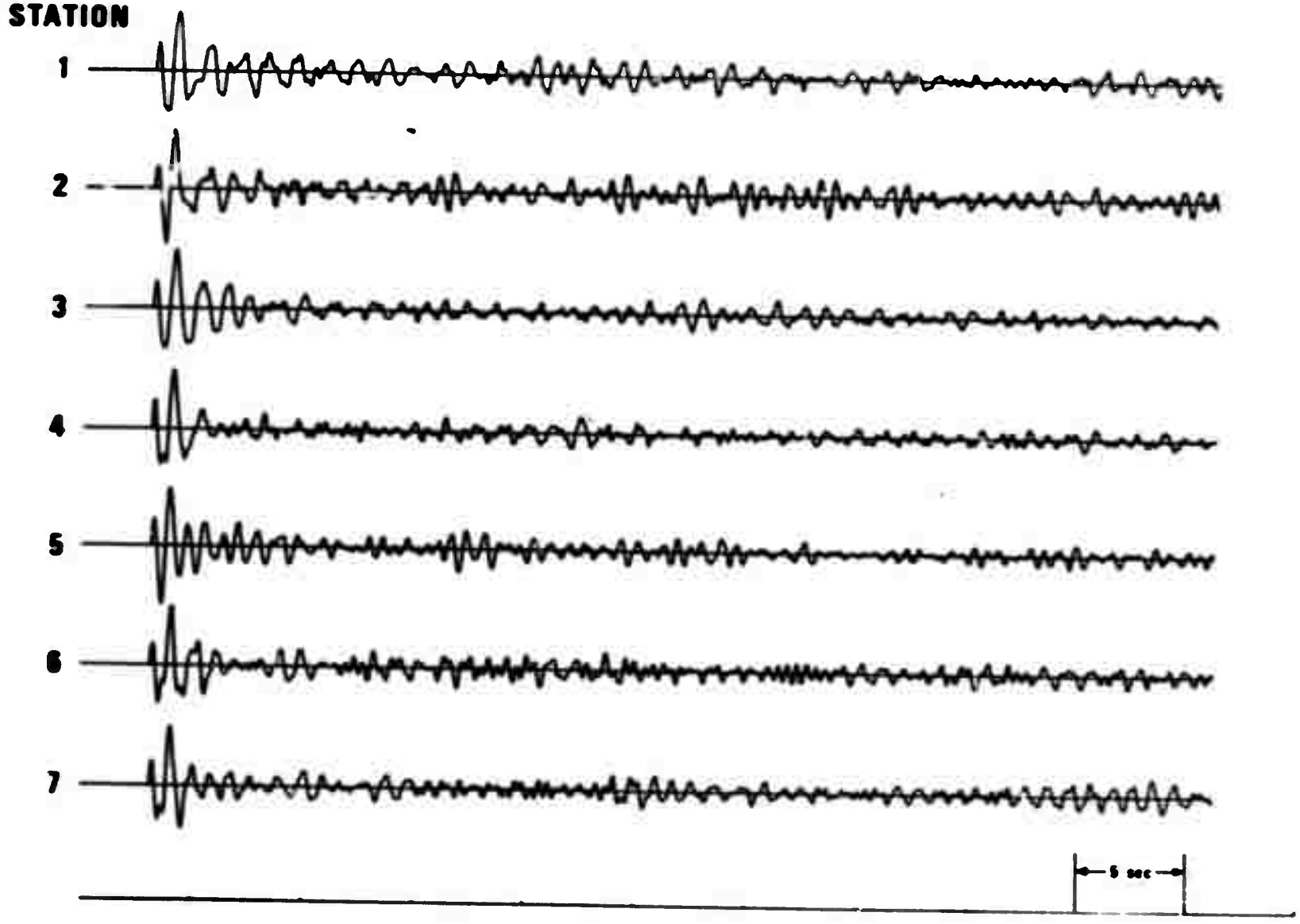

Figure . Theoretical station seismograms, Shot 3.

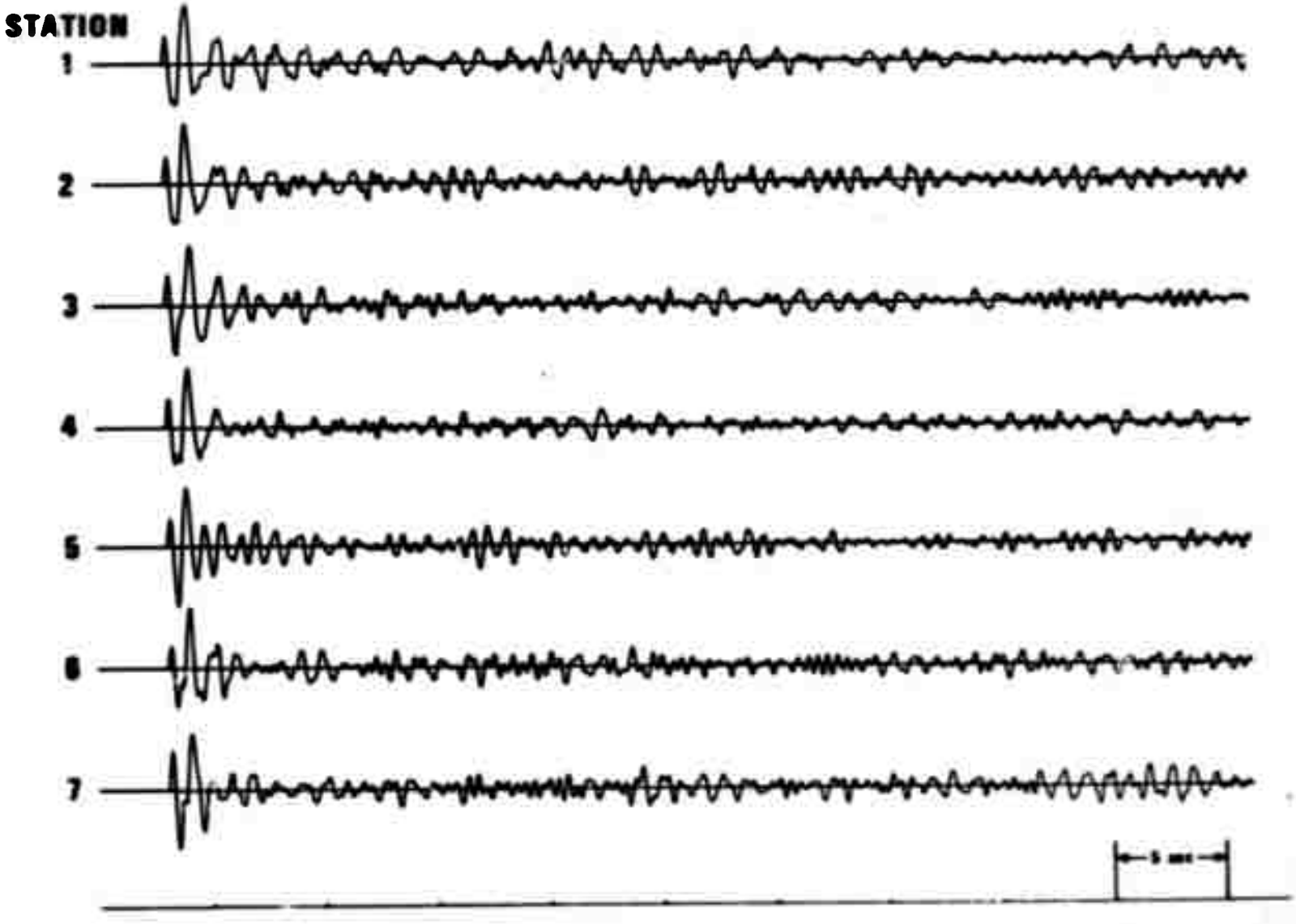

Figure 12. Theoretical staion seismograms, Shot 4.

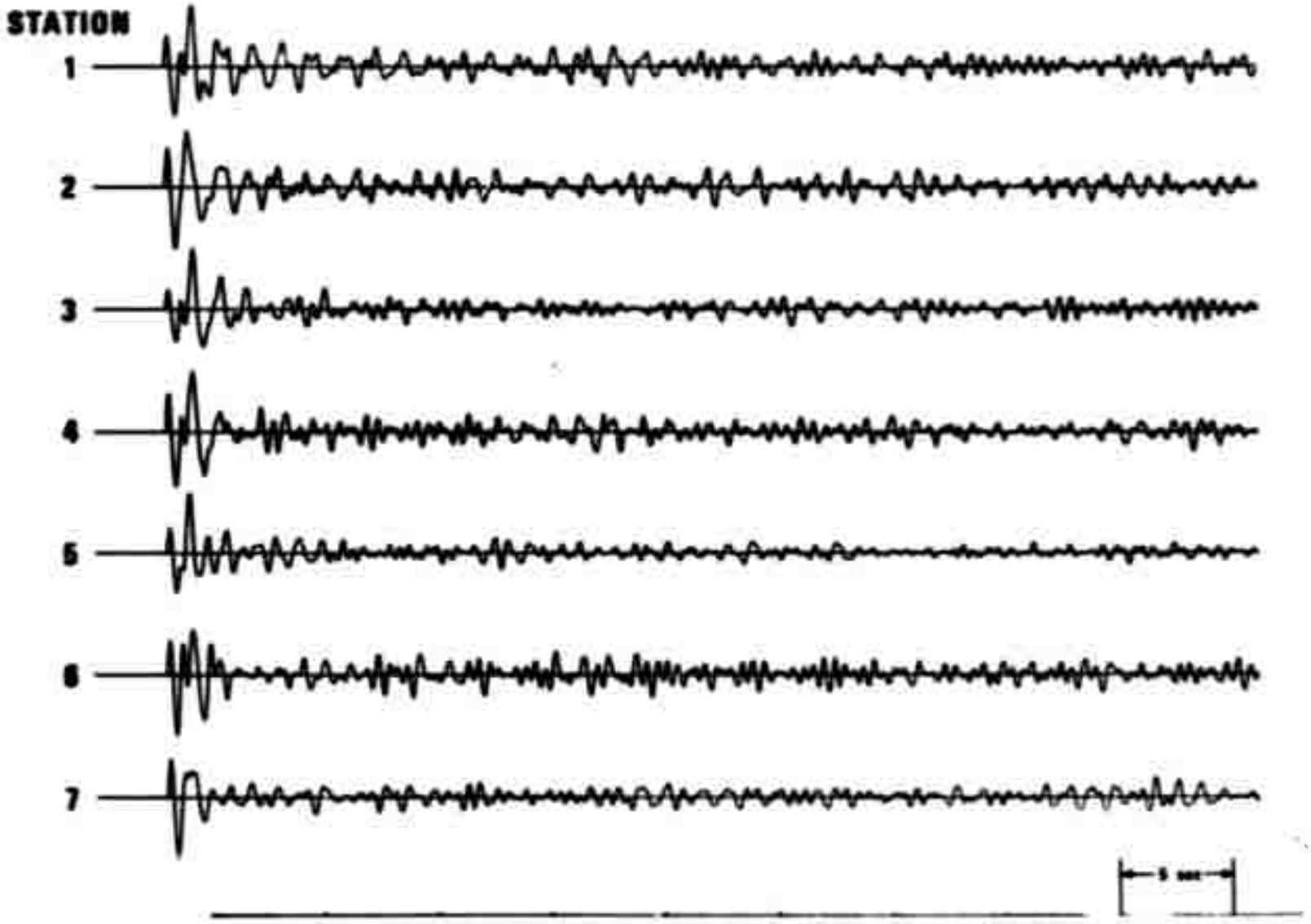

Figure 13. Theoretical station seismograms, Shot 5.

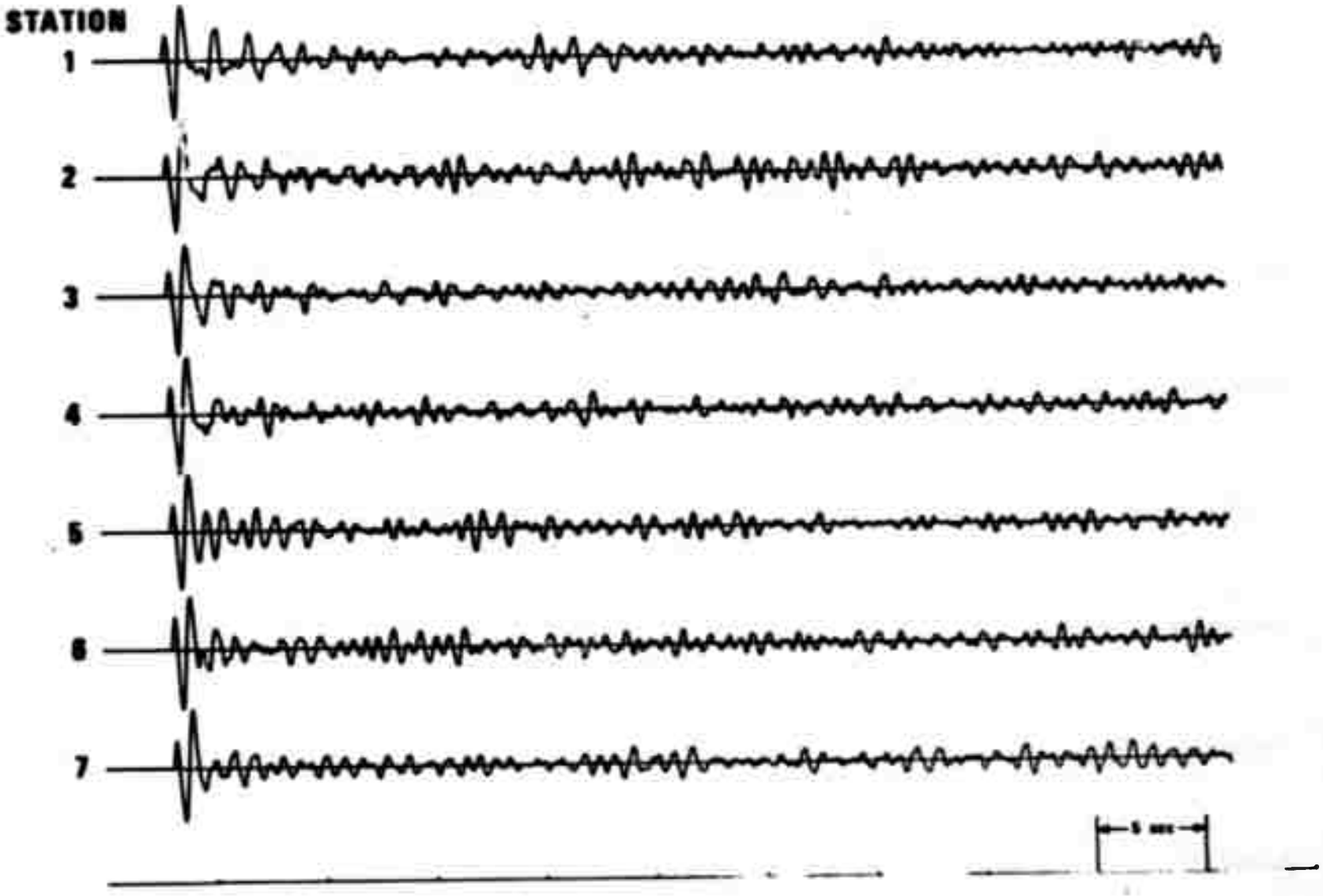

Figure 14. Theoretical station seismograms, Shot 6.

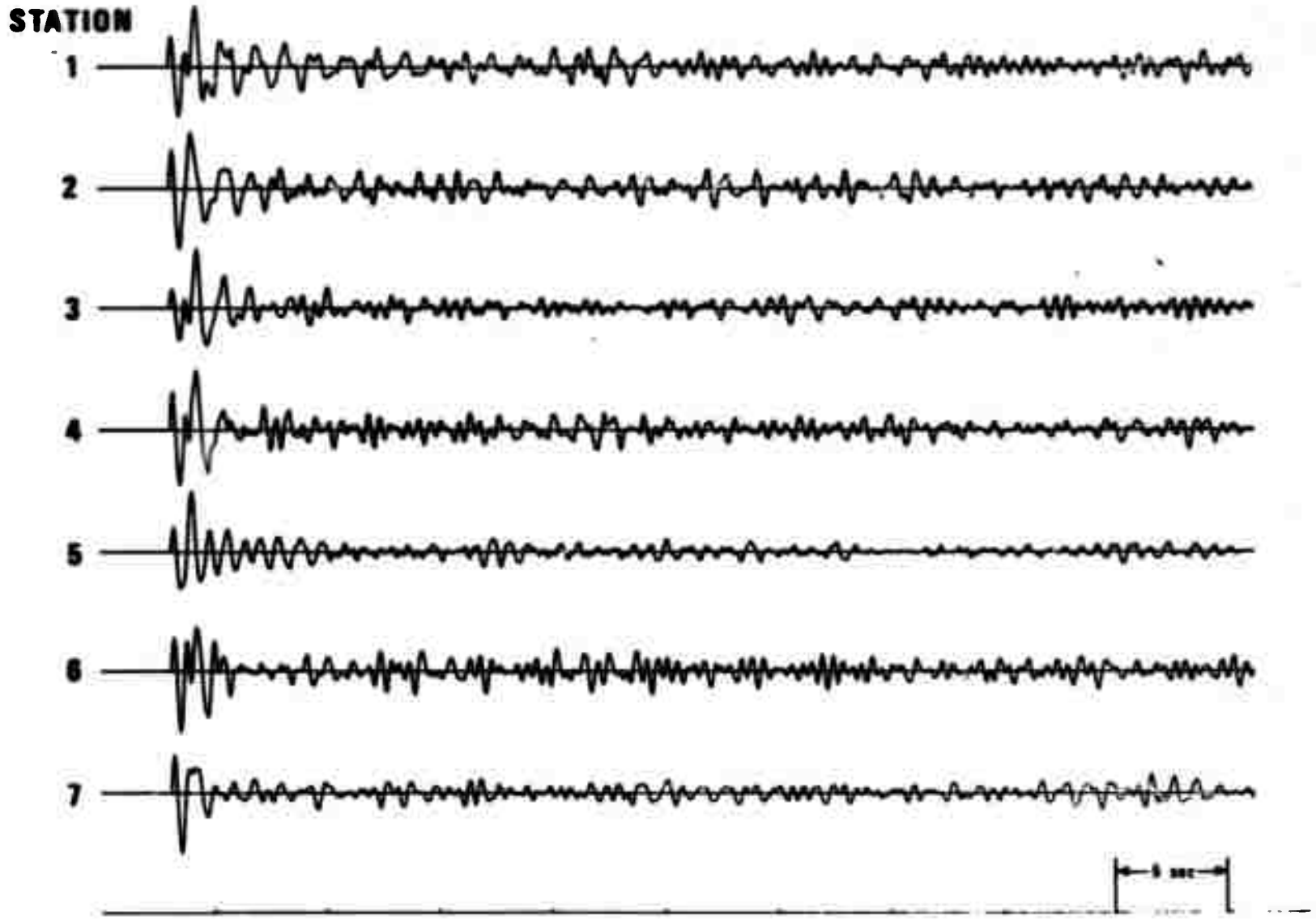

Figure 15. Theoretical station seismogram, Shot 7.

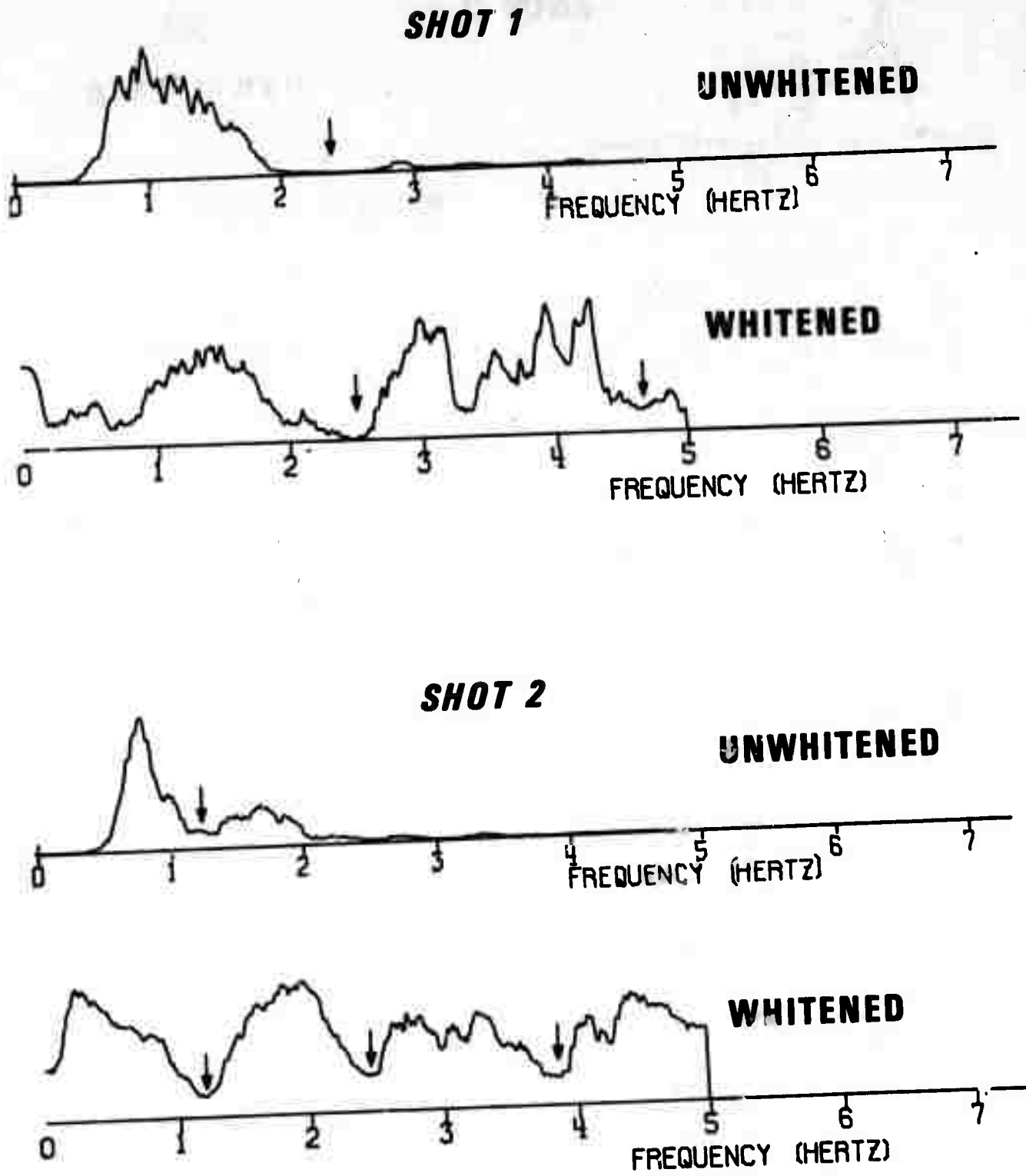

Figure 16. Network-summed spectra, Shots 1 and 2.

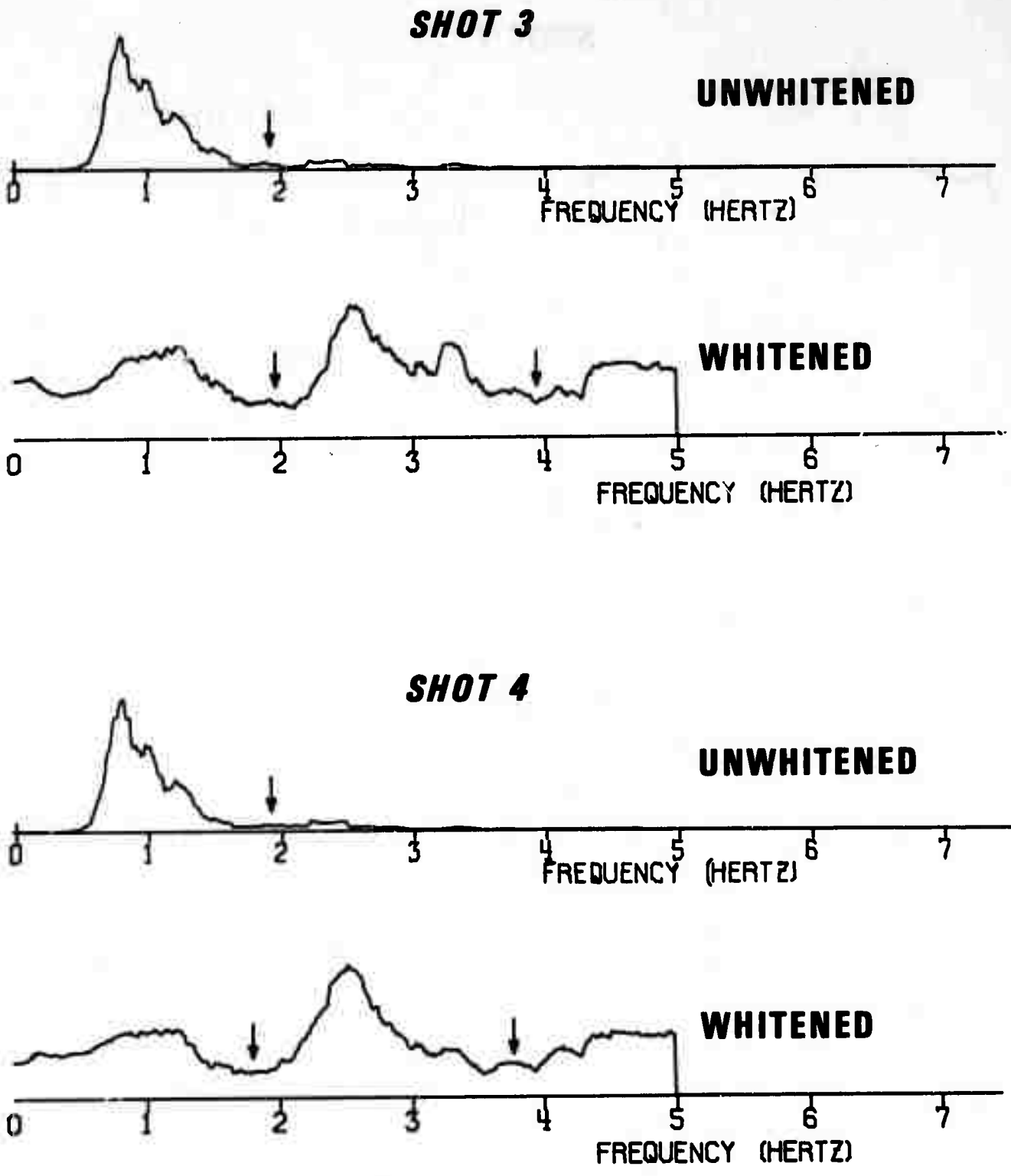

Figure 17. Network-summed spectra, Shots 3 and 4.

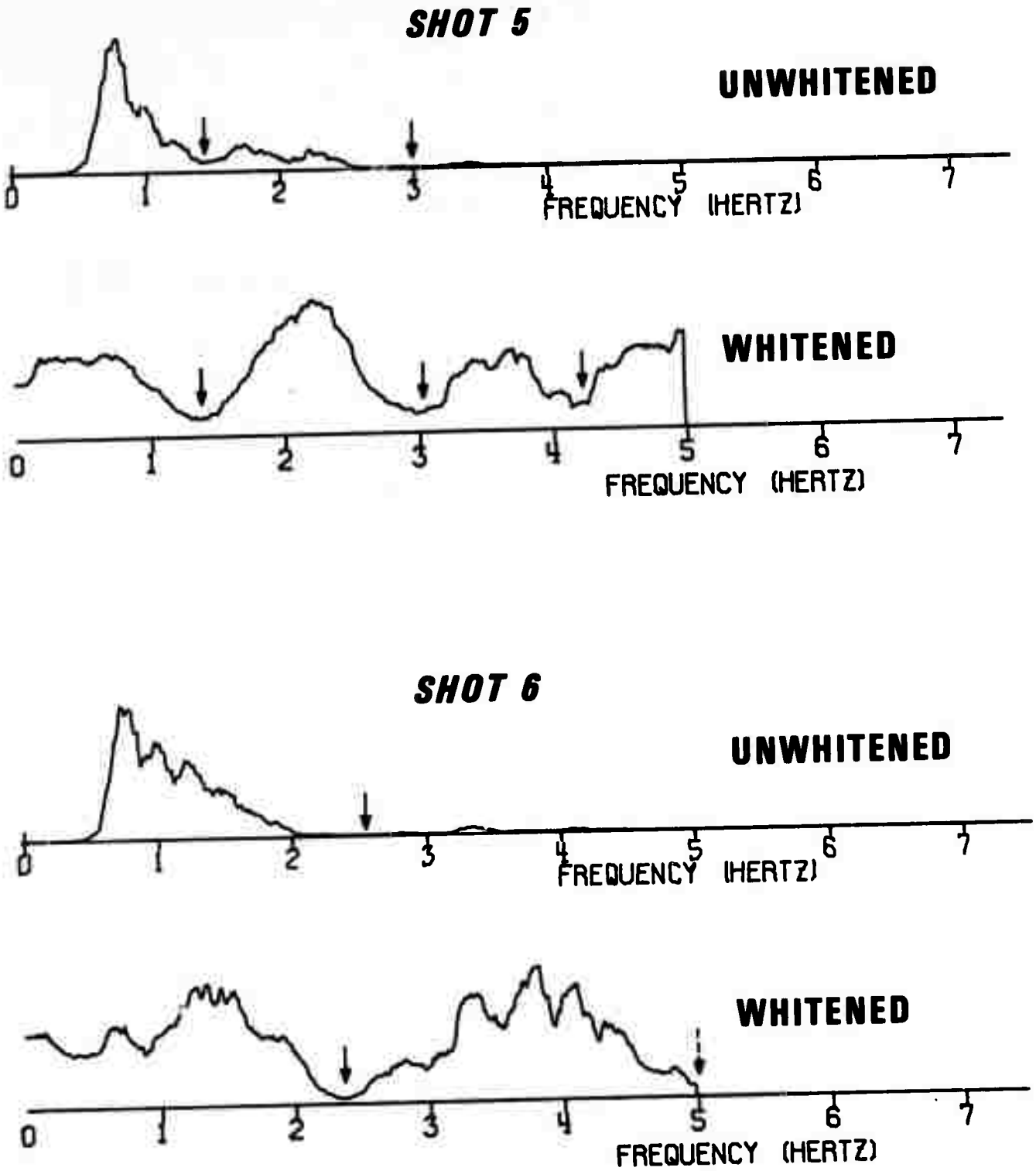

Figure 18. Network-summed spectra, Shots 5 and 6.

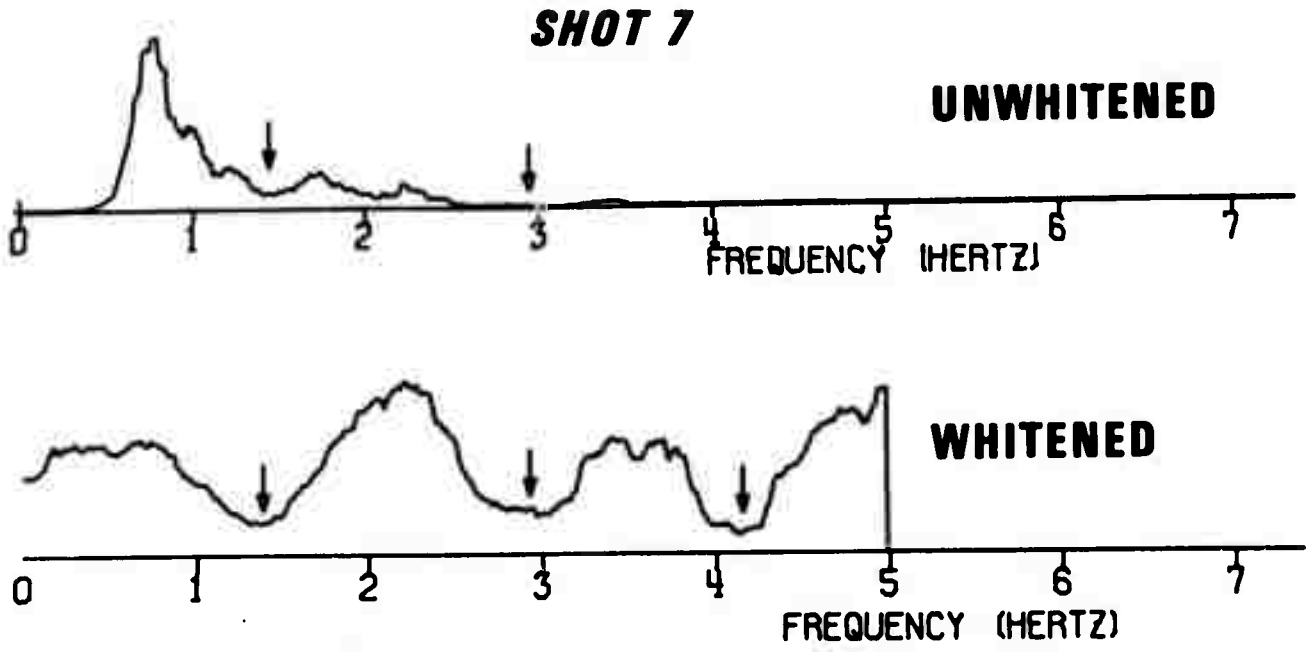

Figure 19. Network-summed spectra, Shot 7.

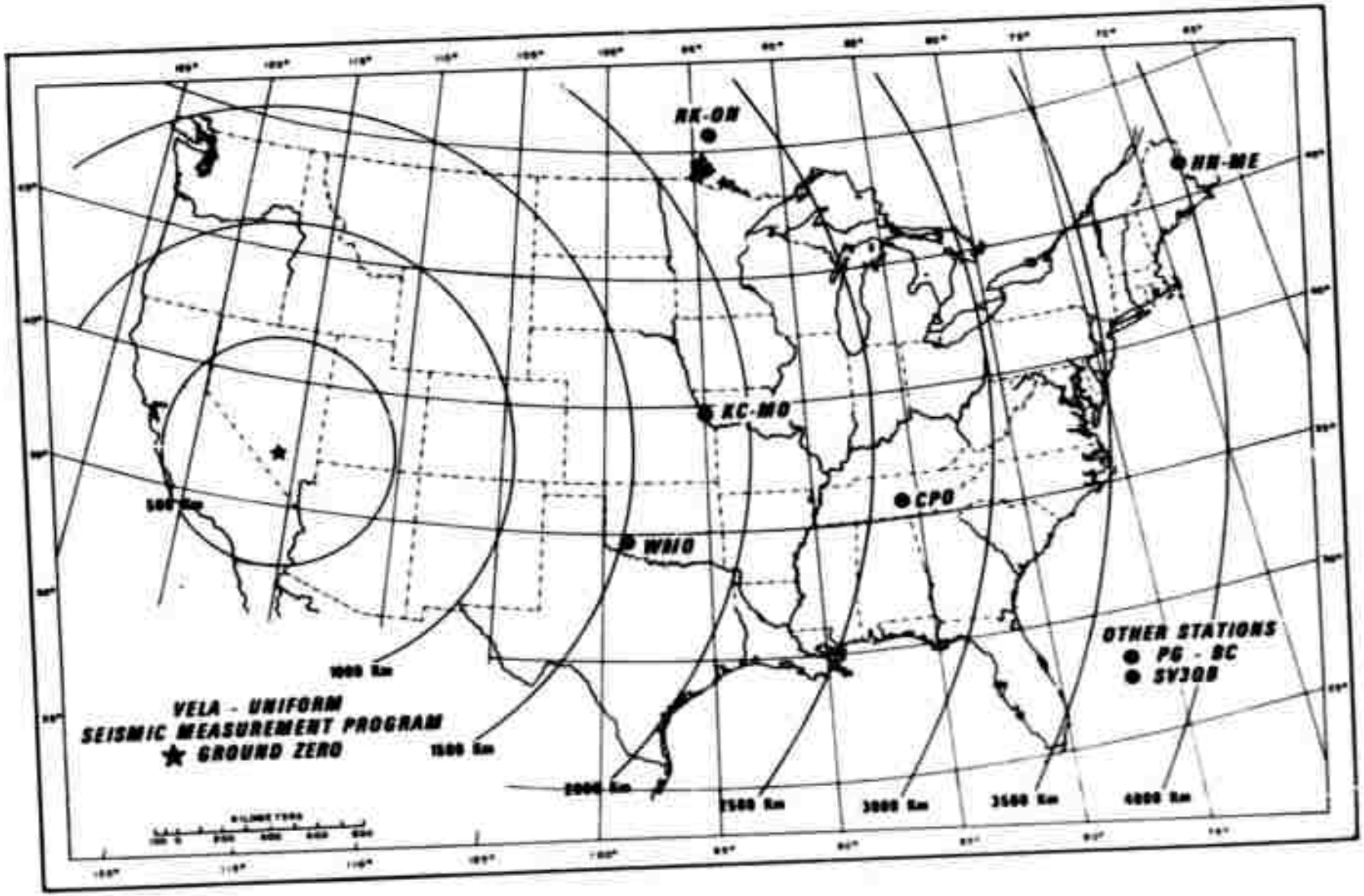

Figure 20. Recording stations.

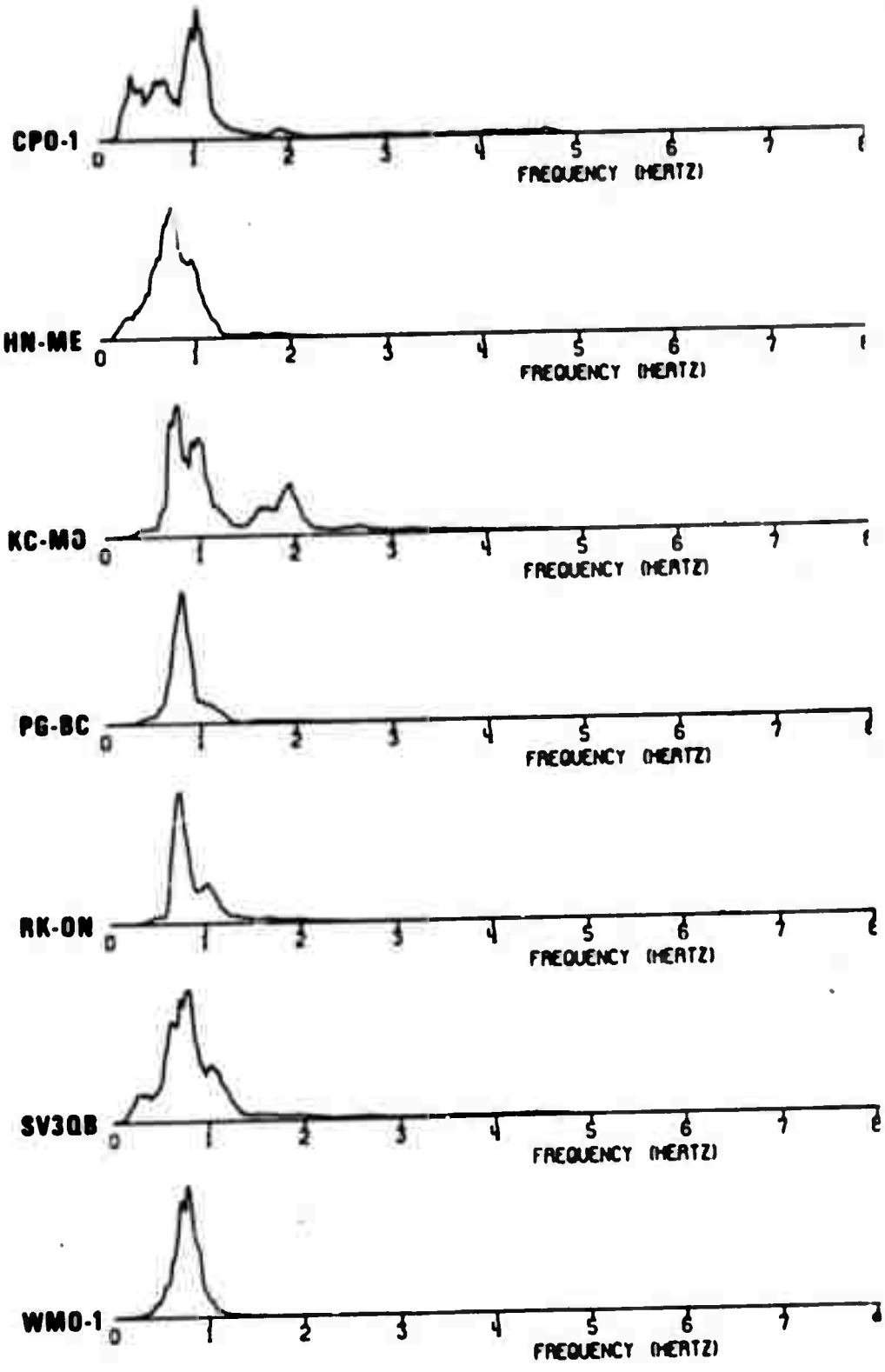

Figure 21. Sum spectra at individual recording stations formed by summing over shots.

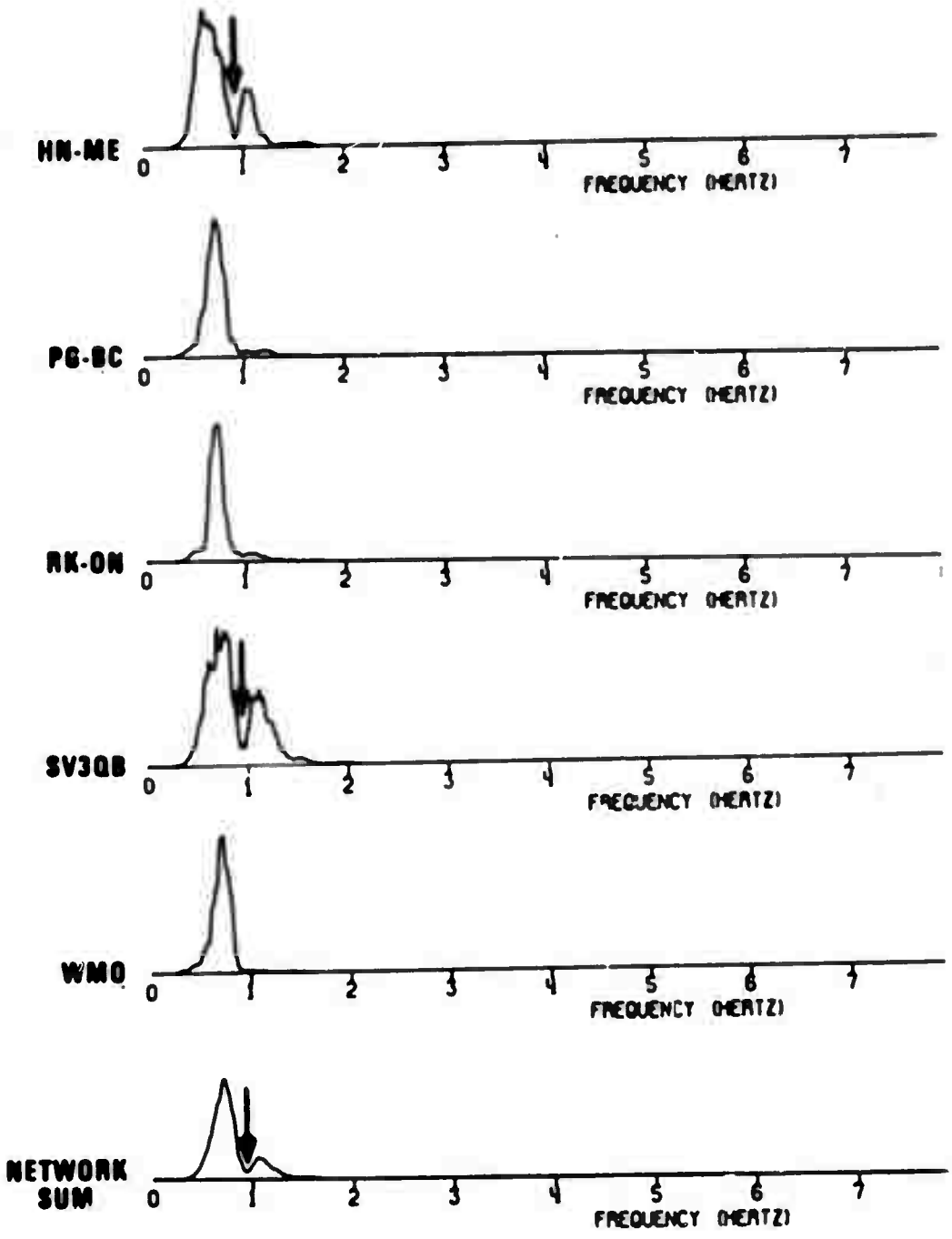

Figure 22. Unwhitened station and network-summed spectra -- BOXCAR.

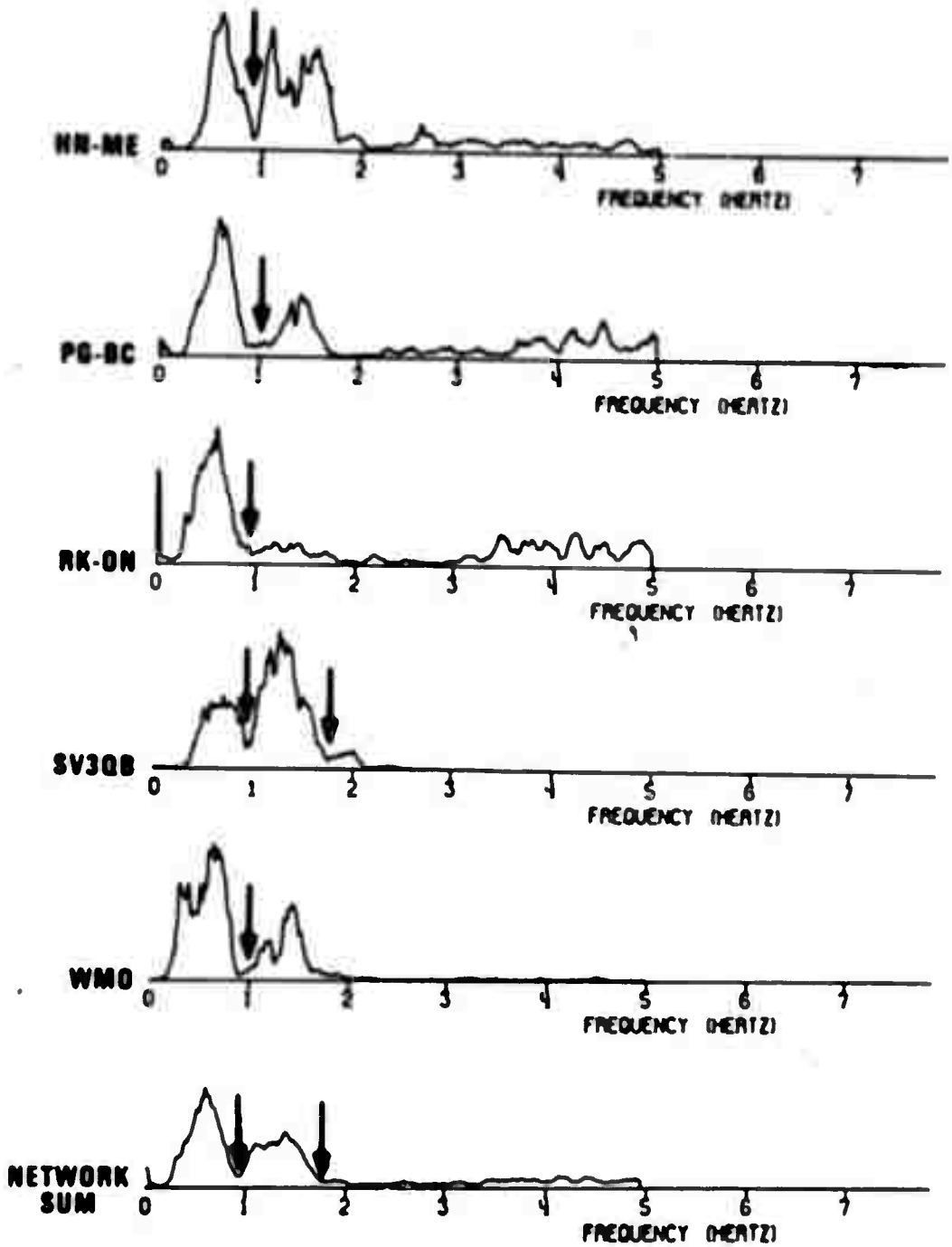

Figure 23. Whitened station and network summed spectra -- BOXCAR.

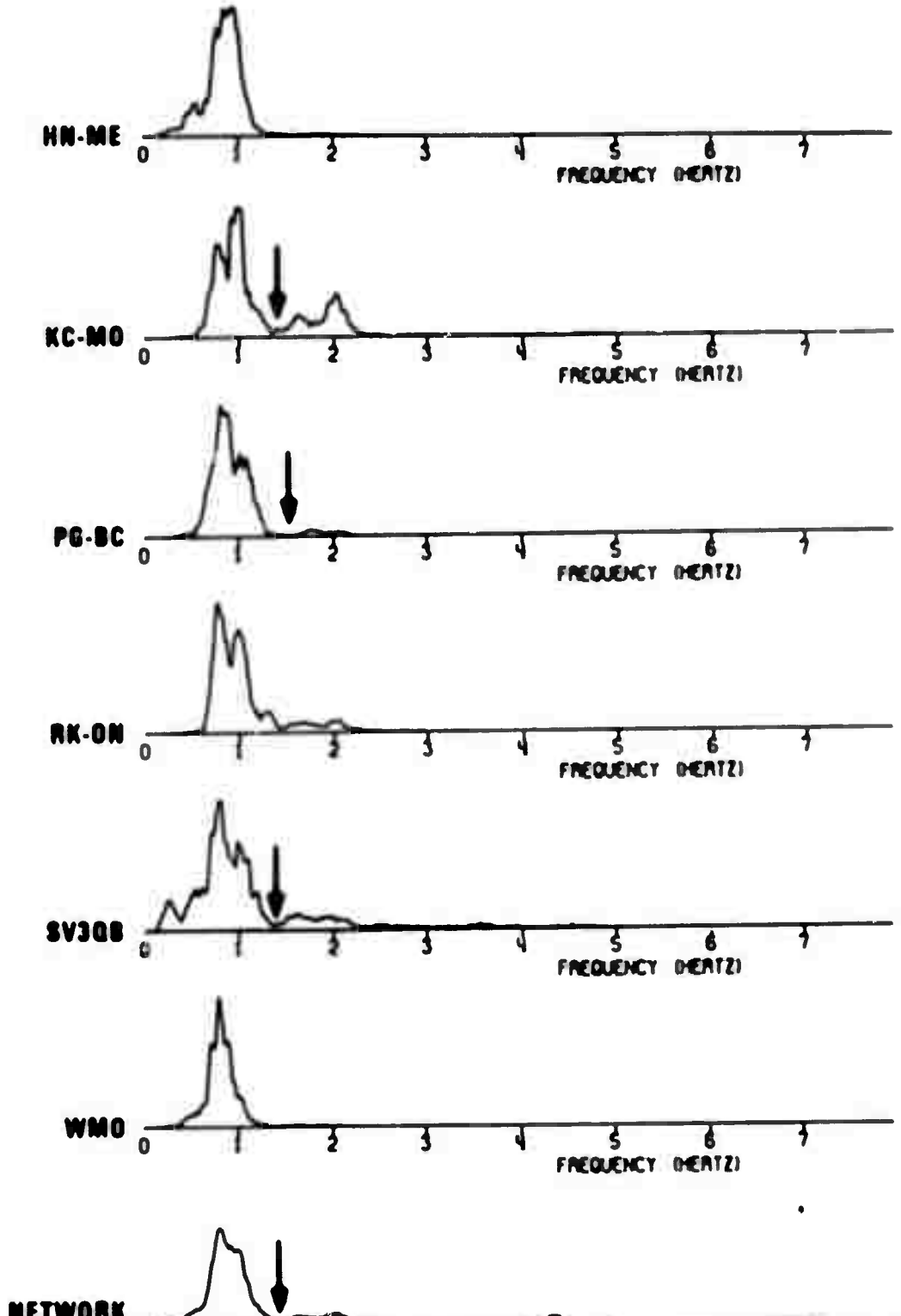

Figure 24. Unwhitened station and network-summed spectra -- CHARTREUSE.

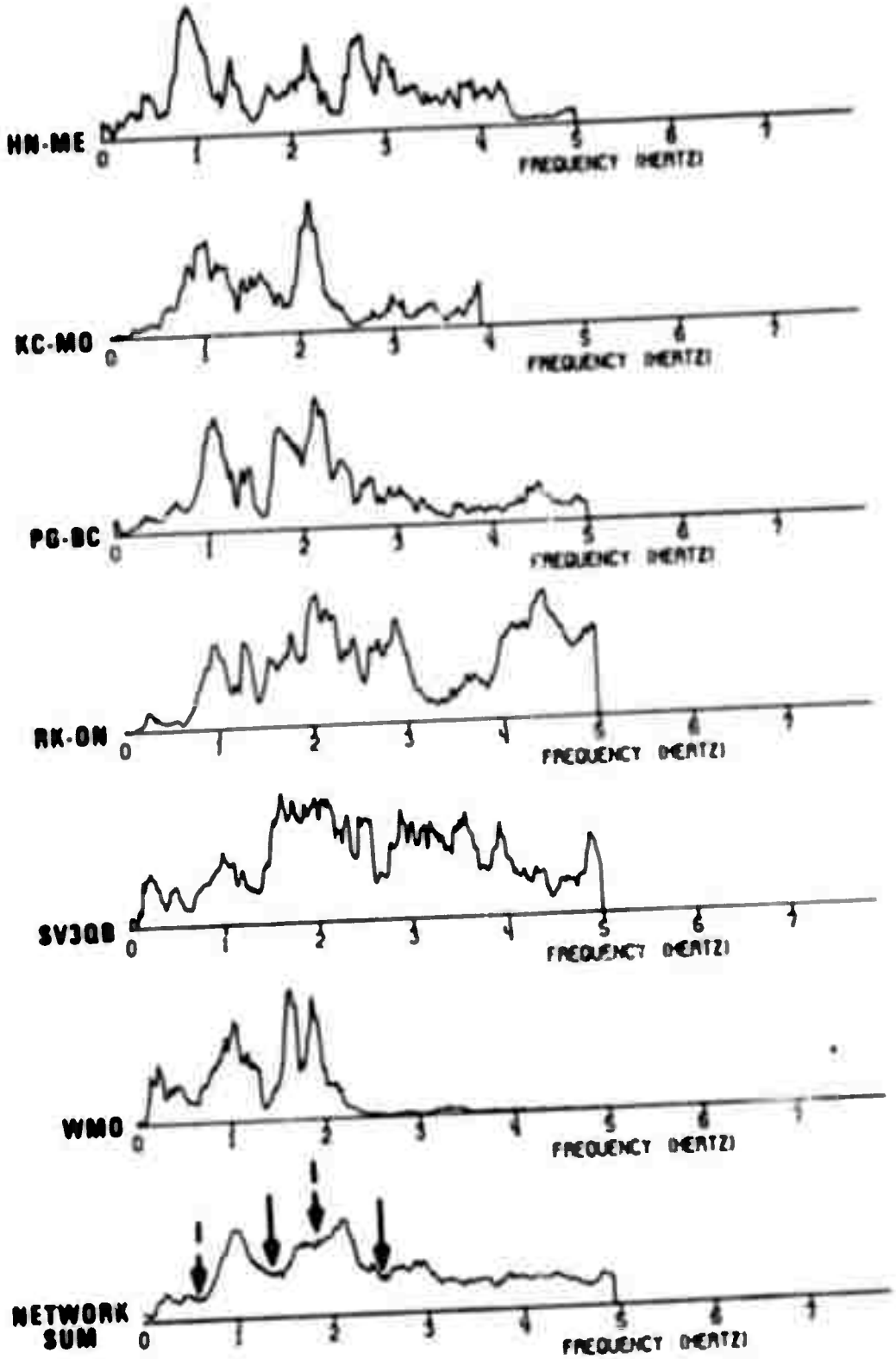

Figure 25. Whitened station and network-summed spectra -- CHARTREUSE.

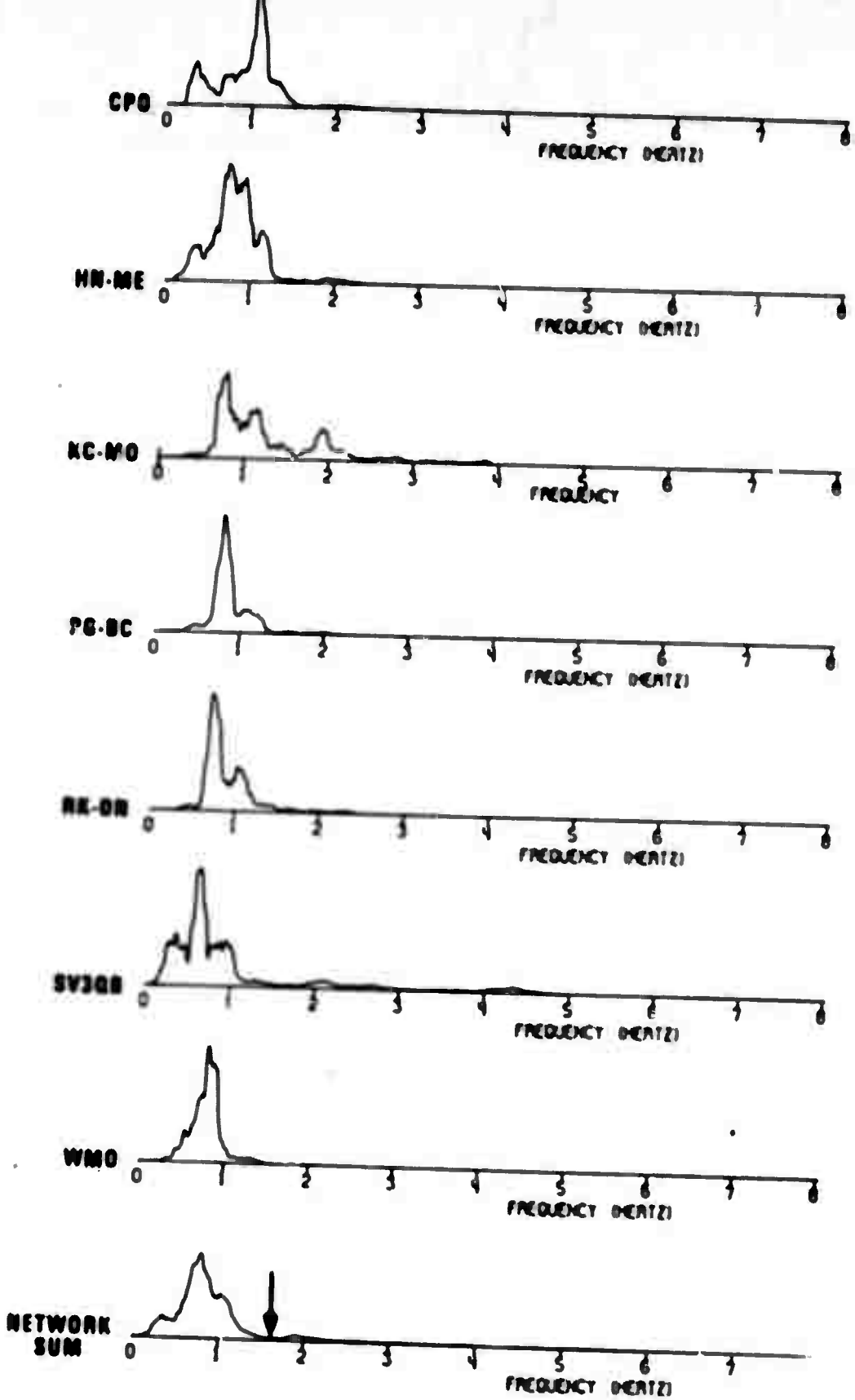

Figure 26. Unwhitened station and network-summed spectra -- DURYEA.

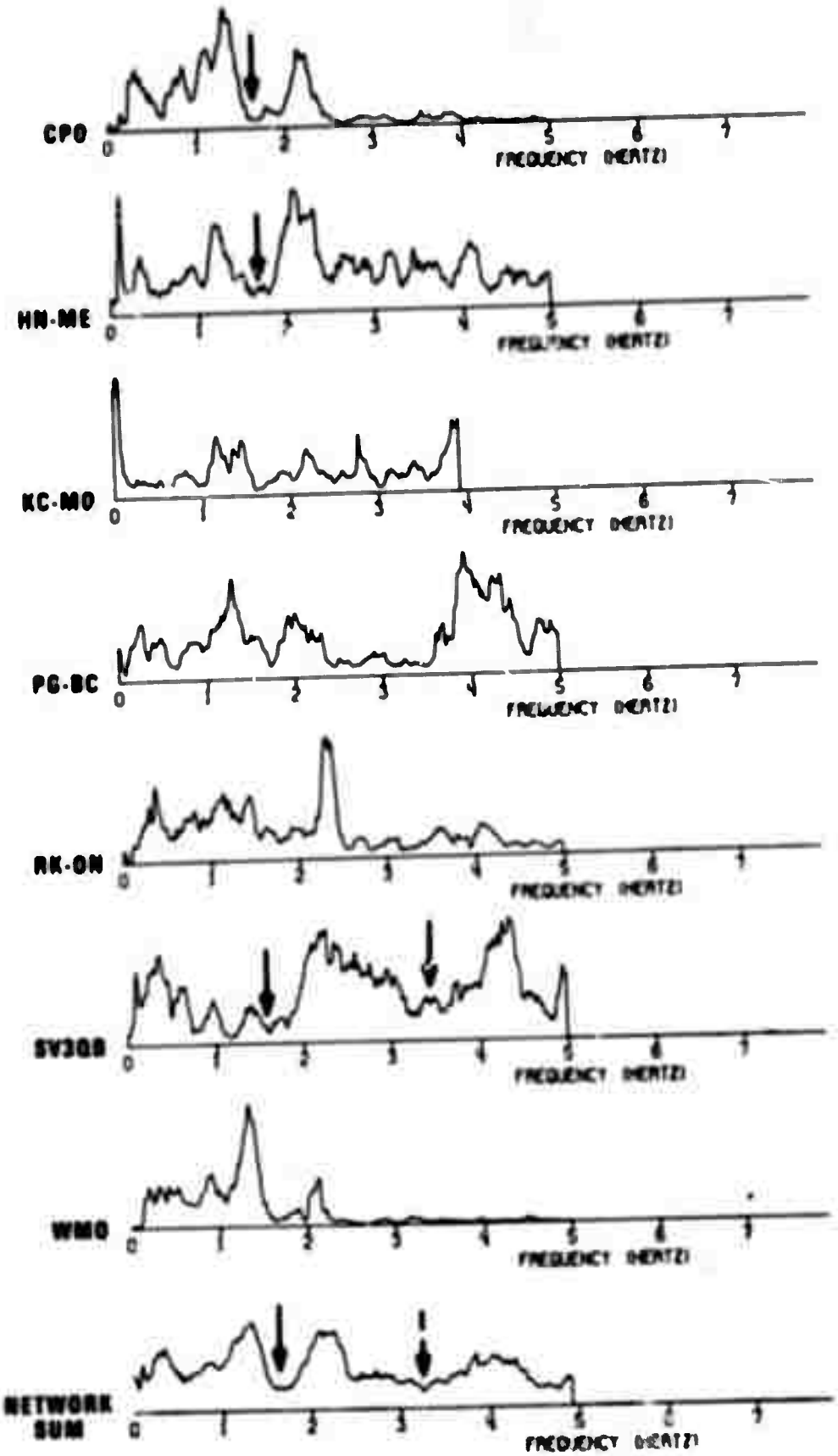

Figure 27. Whitened station and network-summed spectra -- DURYEA.

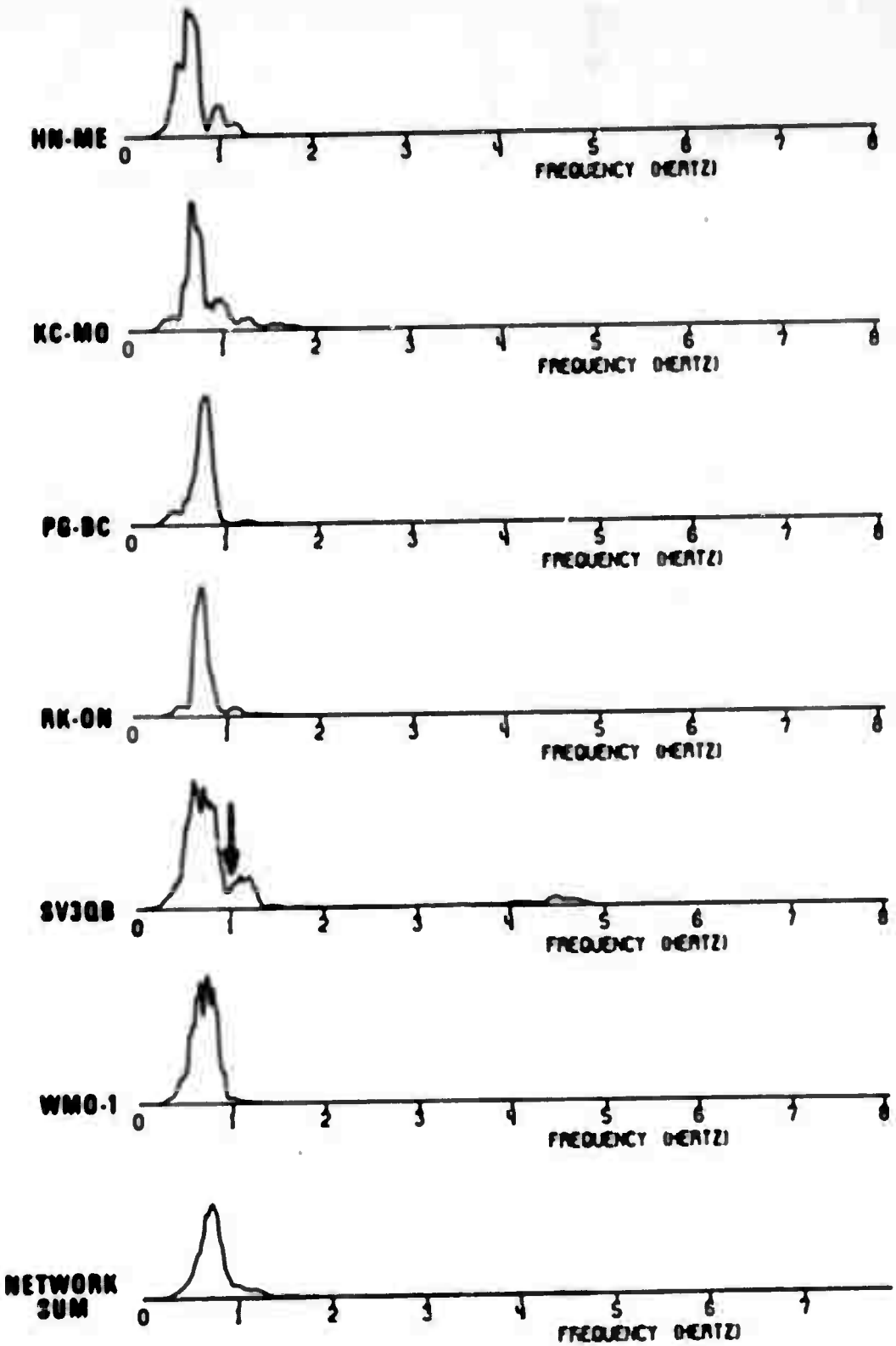

Figure 28. Unwhitened station and network-summed spectra -- GREELEY.

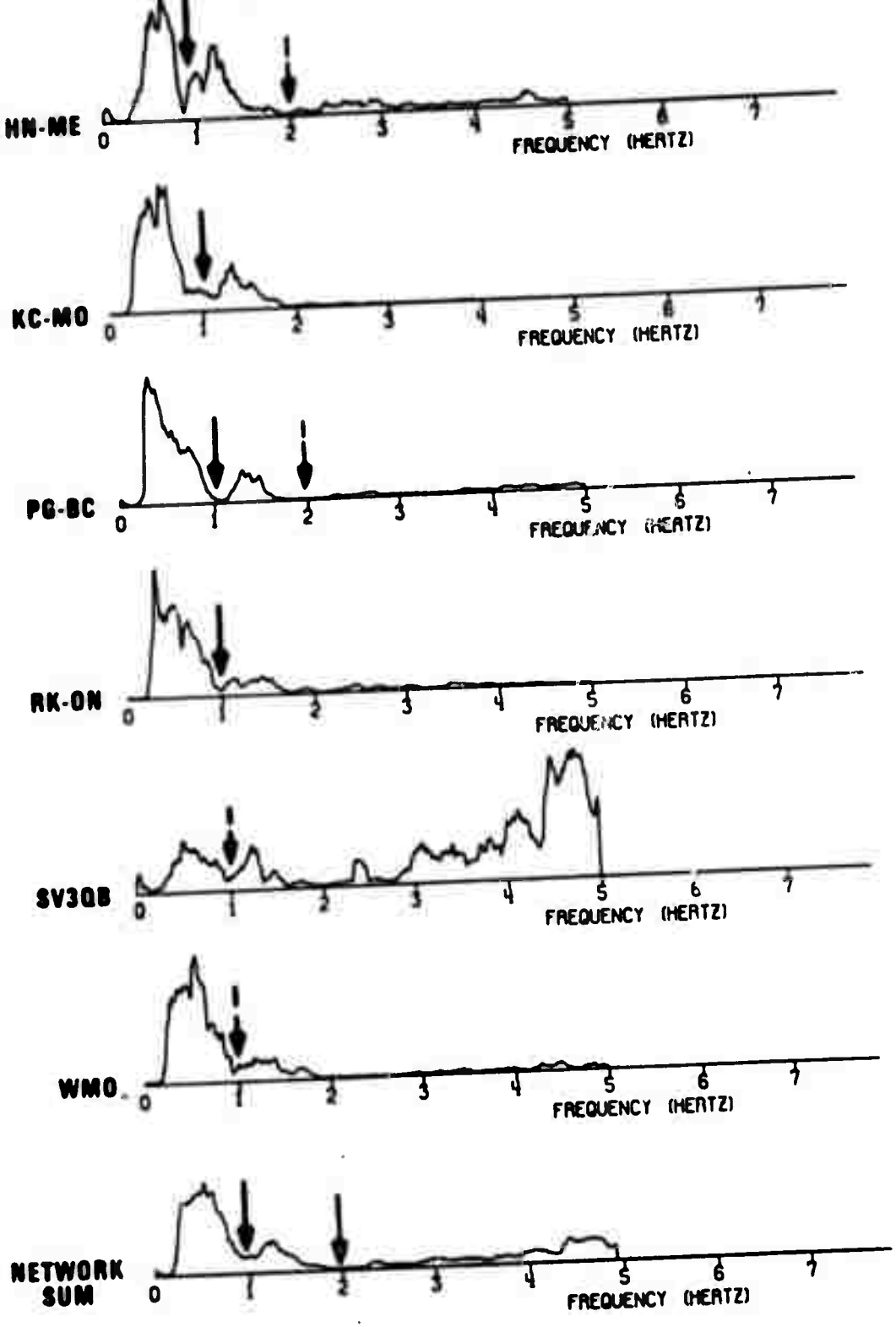

Figure 29. Whitened station and network-summed spectra -- GREELEY.

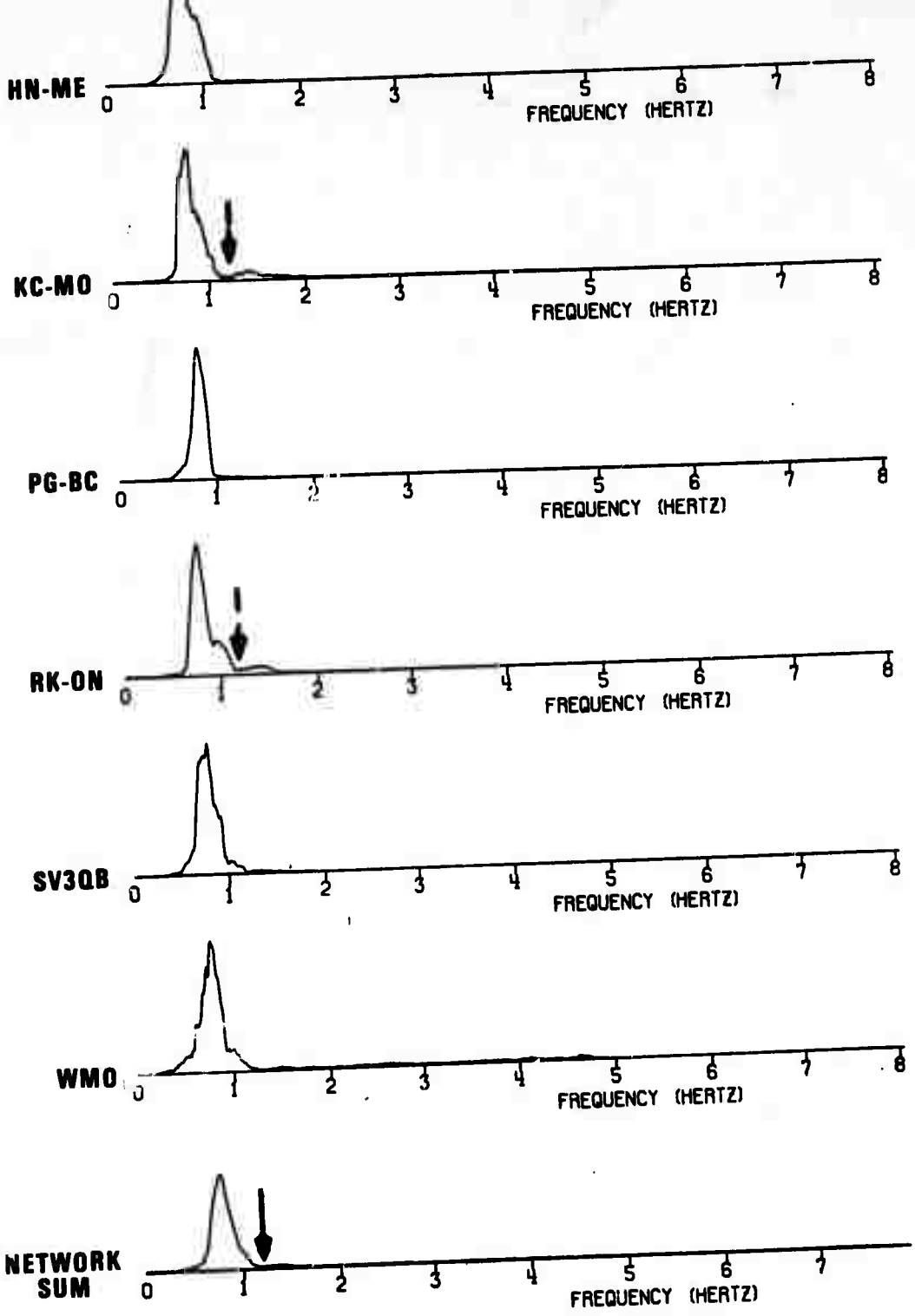

Figure 30. Unwhitened station and network-summed spectra -- HALF BEAK.

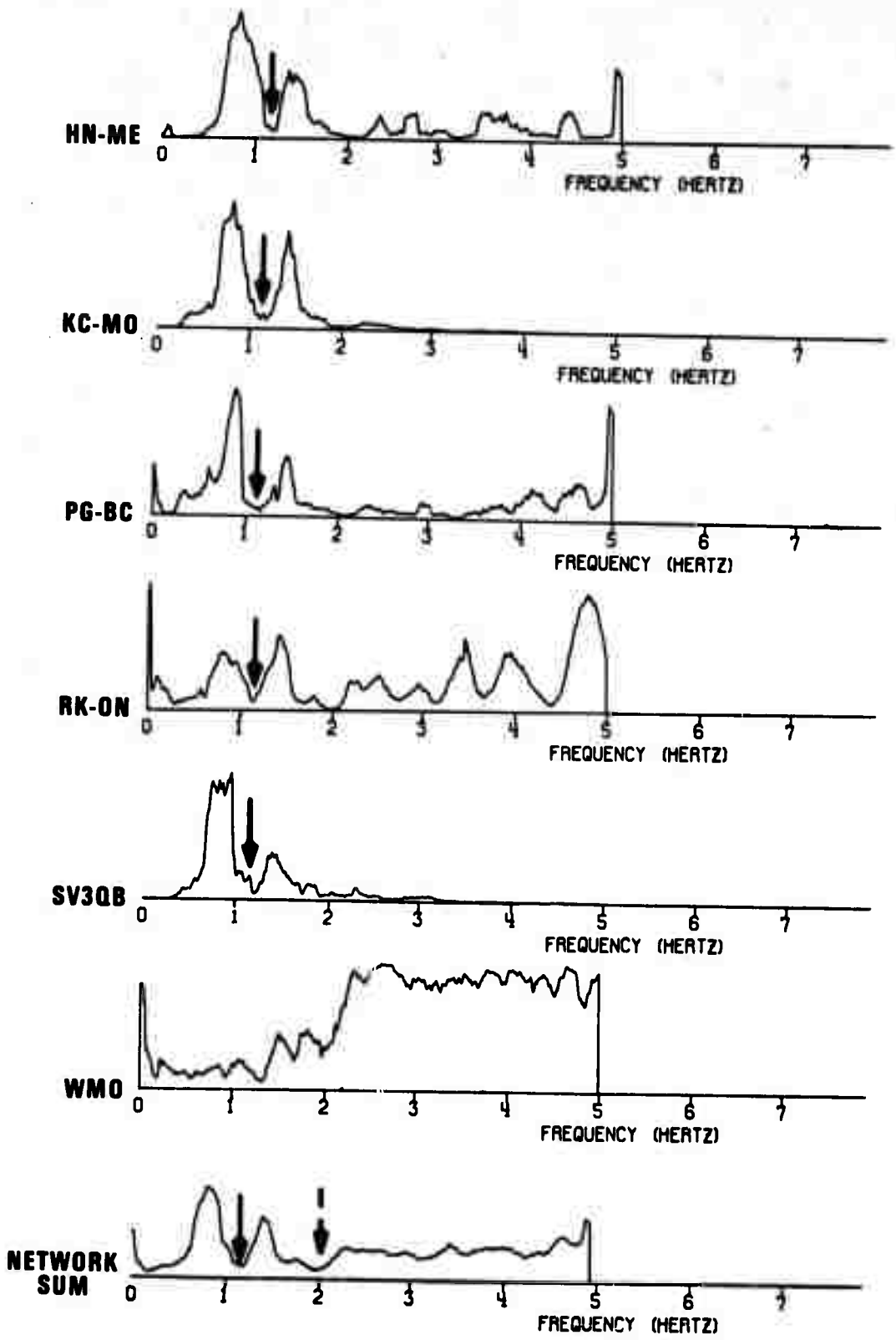

Figure 31. Whitened station and network-summed spectra -- HALF BEAK.

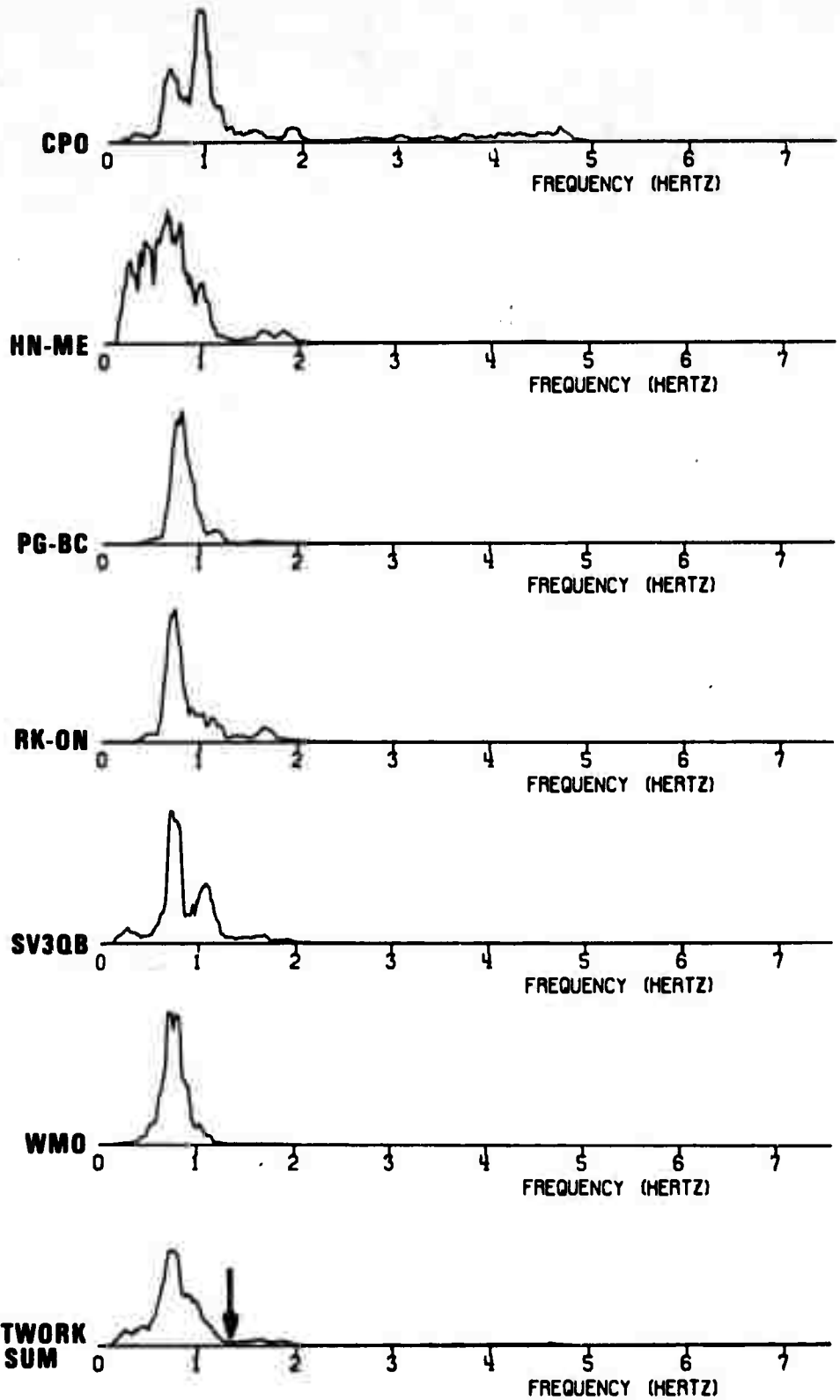

Figure 32. Unwhitened station and network-summed spectra -- KNICKERBOCKER.

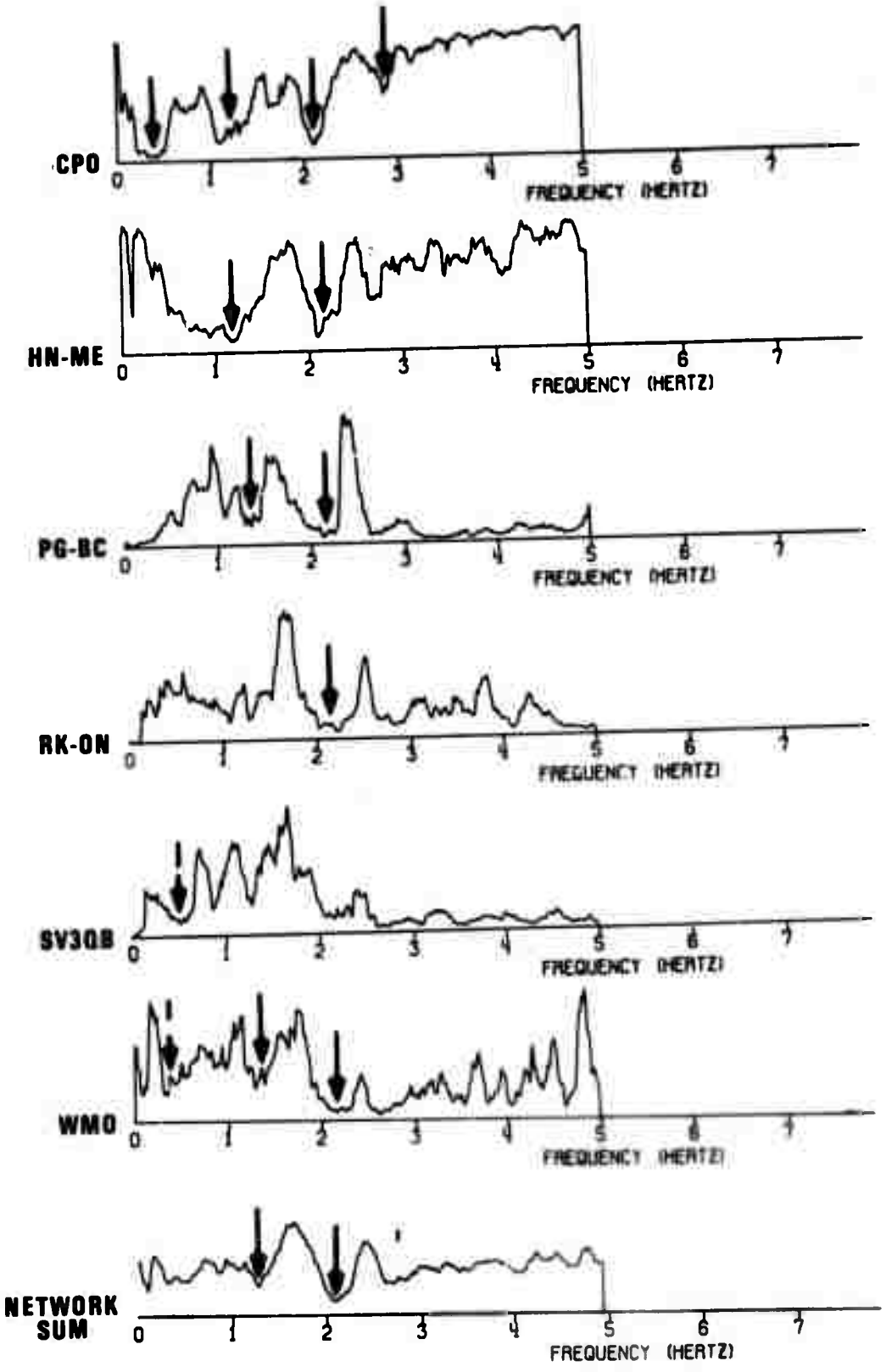

Figure 33. Whitened station and network-summed spectra -- KNICKERBOCKER.

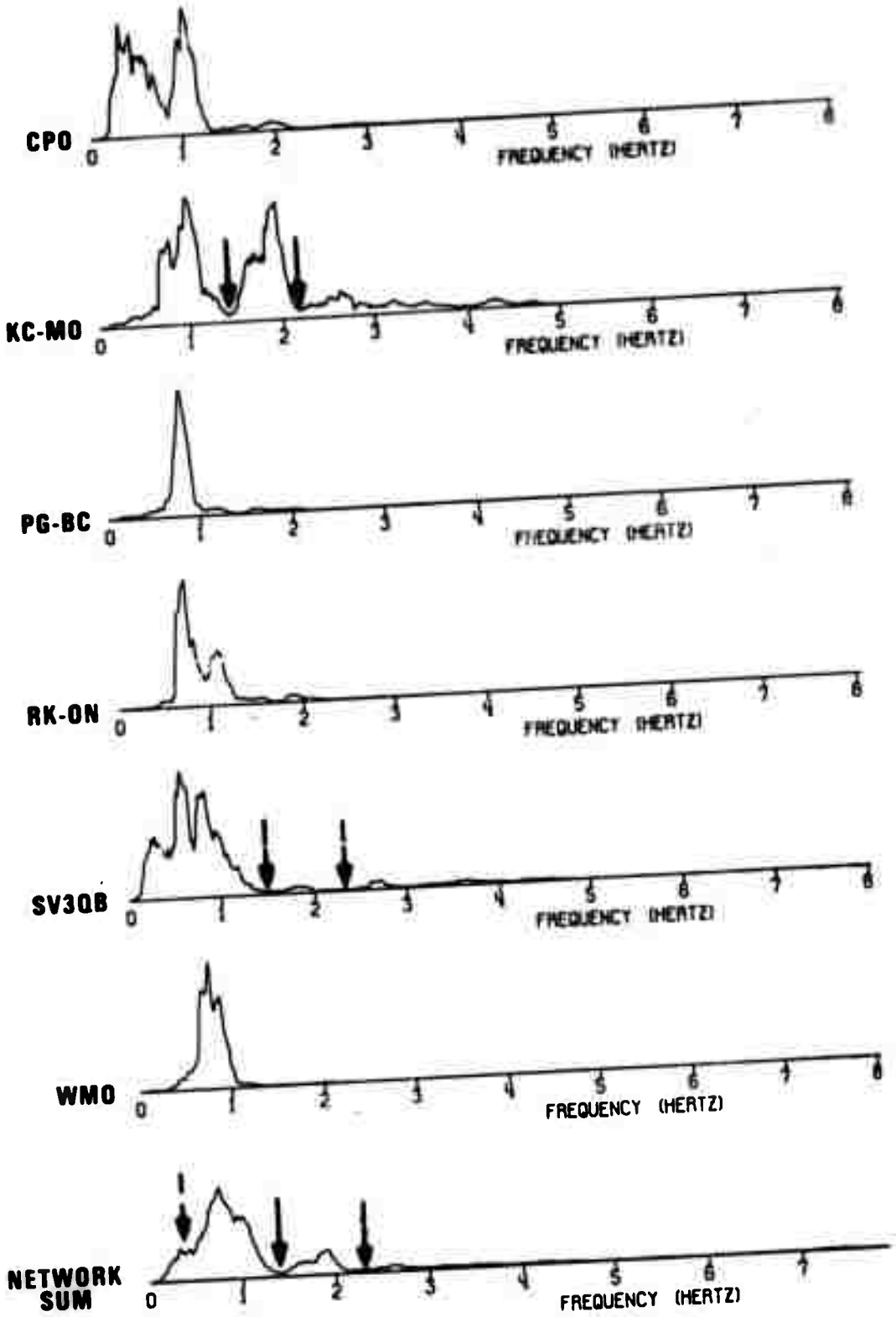

Figure 34. Unwhitened station and network-summed spectra -- REX.

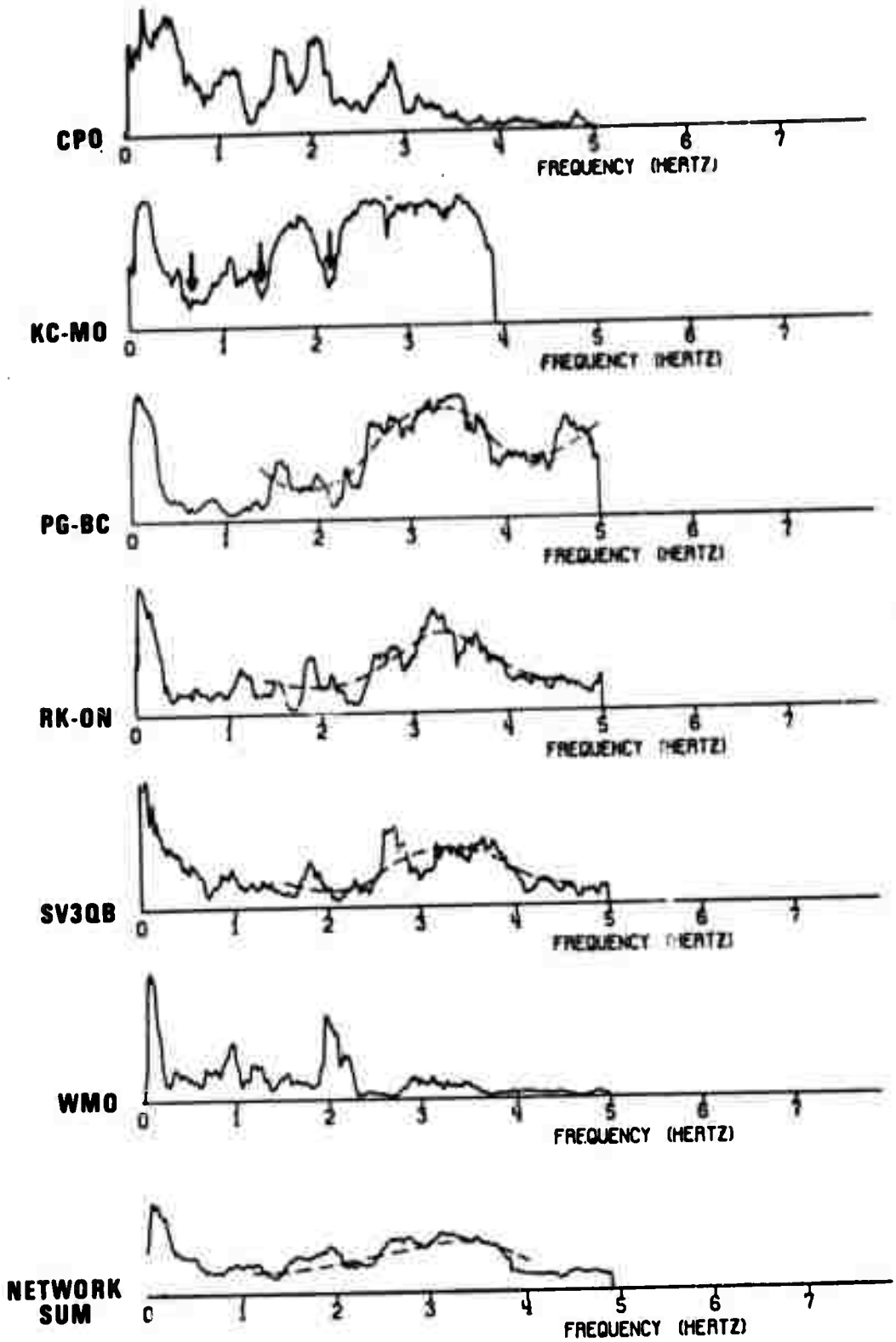

Figure 35. Whitened station and network-summed spectra -- REX.

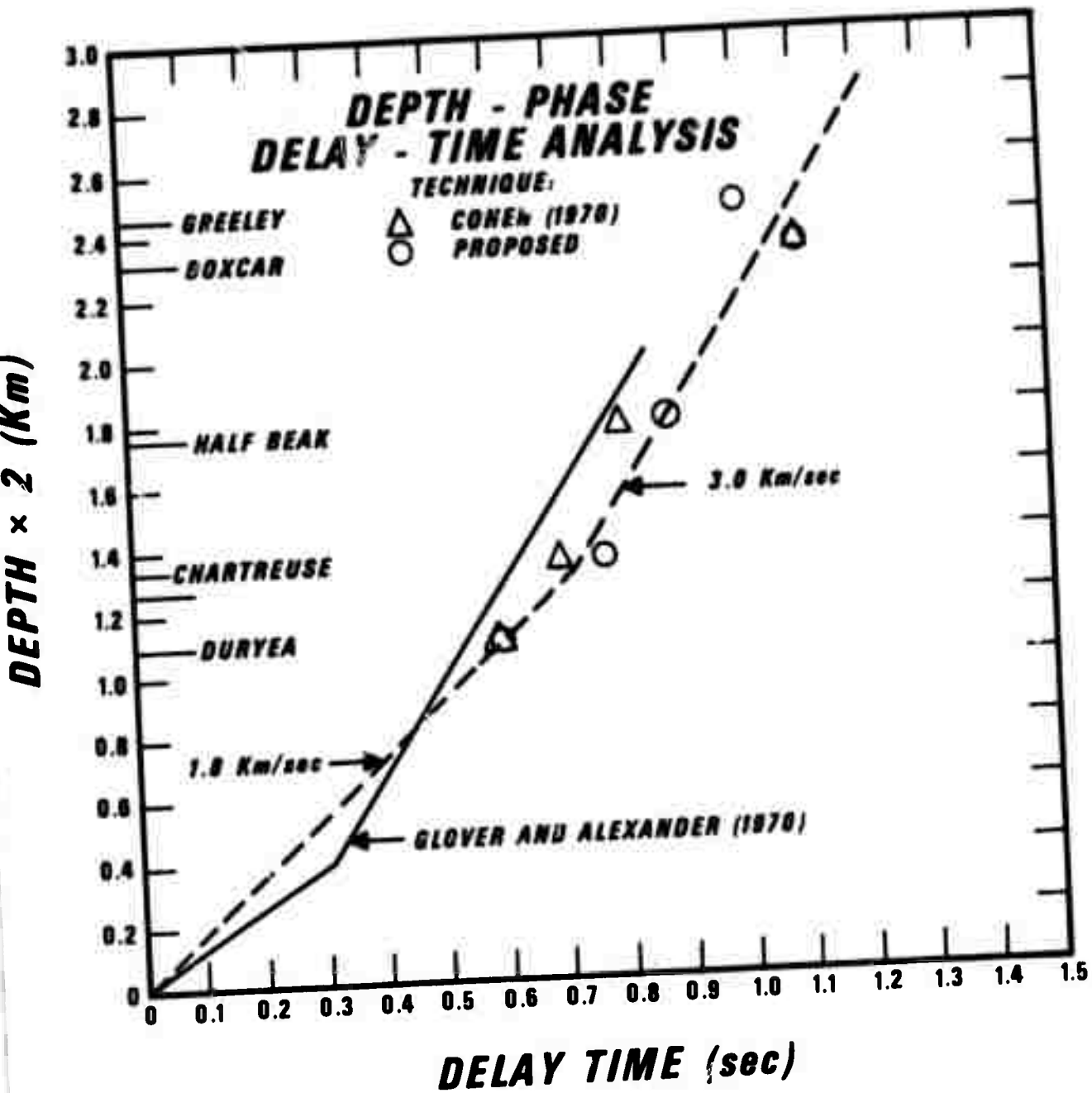

Figure 36. Depth phase time-delay analysis.

APPENDIX

EARTHQUAKE SPECTRA

An analysis of the network-summed spectra for 17 earthquakes recorded at teleseismic distances (Table I) indicates that the spectra for six events exhibited spectral nulls which may be related to interference of the type pP-P. Examples of these spectra are given in Figure 1. Instrument response was removed from the individual station spectra prior to network averaging.

If we interpret the null at 1.7 Hz in the spectrum of the 16 March 1964 Kurile Island event as being the first depth phase null, the data imply a pP delay time of 0.6 seconds. Assuming an over-burden velocity of 3 km/sec, this delay time then yields a source depth estimate of 0.9 km. A similar argument applied to the broad band null at 2.5 Hz in the spectrum for the 25 April 1964 Kuriles event suggests a source depth of 0.6 km. Neither can be considered correct in view of the depth estimates of 140 and 40 km, respectively, reported for these events.

Spectra shown for the Andreanof Island and Chilean events in Figure 1 are typical of the network-summed earthquake spectra found in this study. For completeness however, network summed spectra for the 14 remaining events studied are shown in Figures 2 through 4.

TABLE I

Principle Facts for Suite of Earthquakes

Event	Date	m_b	Depth (km)	No. Stations Used	Spectral Characteristics
Fallon, Nevada	20 Jul 62	4.4	20	9	Possible nulls at 1.35 and 2.65 Hz (Poor)
Cache Creek	30 Aug 62	5.8	37	21	None
Central Peru	13 Apr 63	6.3	125	16	None
Manchuria	21 Jun 63	4.9	33	12	Nulls at 0.8, 1.0, 1.3, 1.6 Hz
Kamchatka	15 Jul 63	5.2	60	12	None
Sakhalin Is.	07 Aug 63	5.1	33	11	None
Sea of Okhotsk	25 Aug 63	4.7	134	4	None
Kara Sea	08 Oct 63	4.7	25	8	None
Kurile Is.	16 Mar 64	5.7	140	13	Nulls at 1.7 and 2.6 Hz
Kurile Is.	08 Apr 64	5.5	40	12	None
Kurile Is.	25 Apr 64	4.6	80	9	Broad null at 2.5 Hz
Kurile Is.	02 May 64	5.7	35	17	Nulls at 0.9 and 1.25 Hz
Kurile Is.	24 Jul 64	5.9	33	12	None
Andreanoff Is.	22 Nov 65	5.9	40	15	None
New Mexico	23 Jan 66	5.5	10	7	None
Coast of Chile	12 Mar 66	4.9	55	6	None
Mid-Atlantic	14 Mar 66	5.2	33	18	Possible nulls at 1.5 and 3.0 Hz

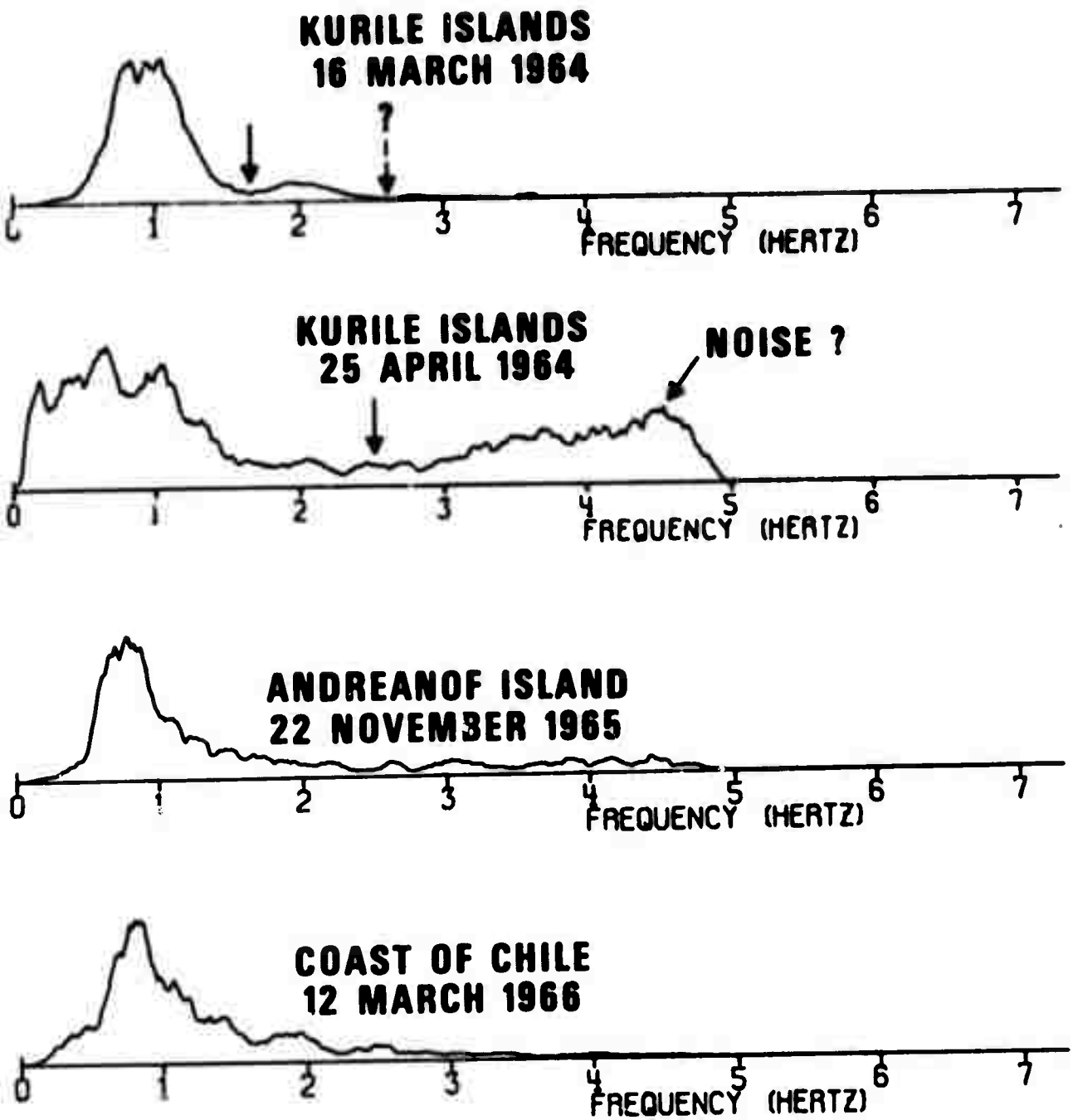

Figure 1. Earthquake spectra network sums.

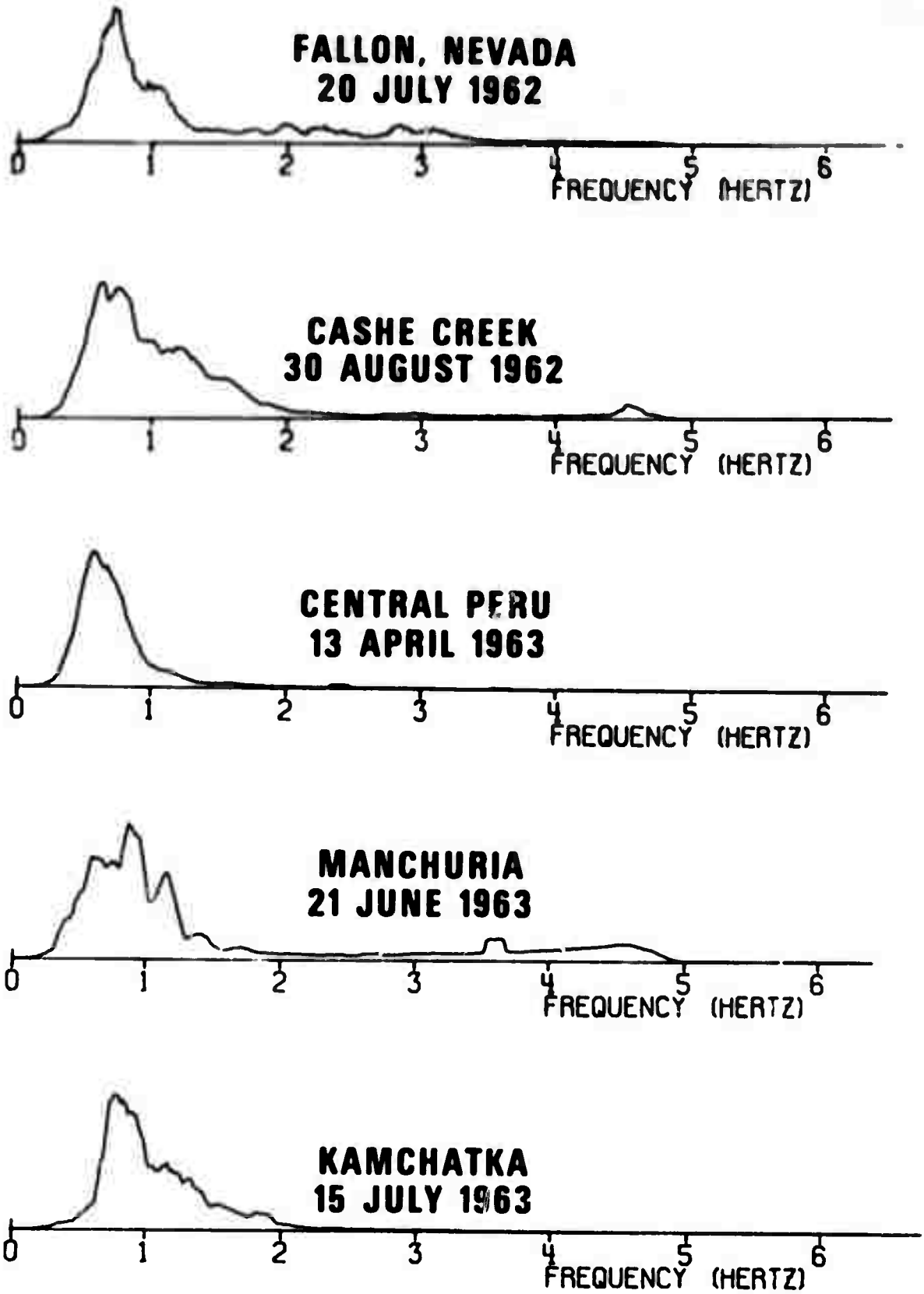

Figure 2. Earthquake spectra network sums.

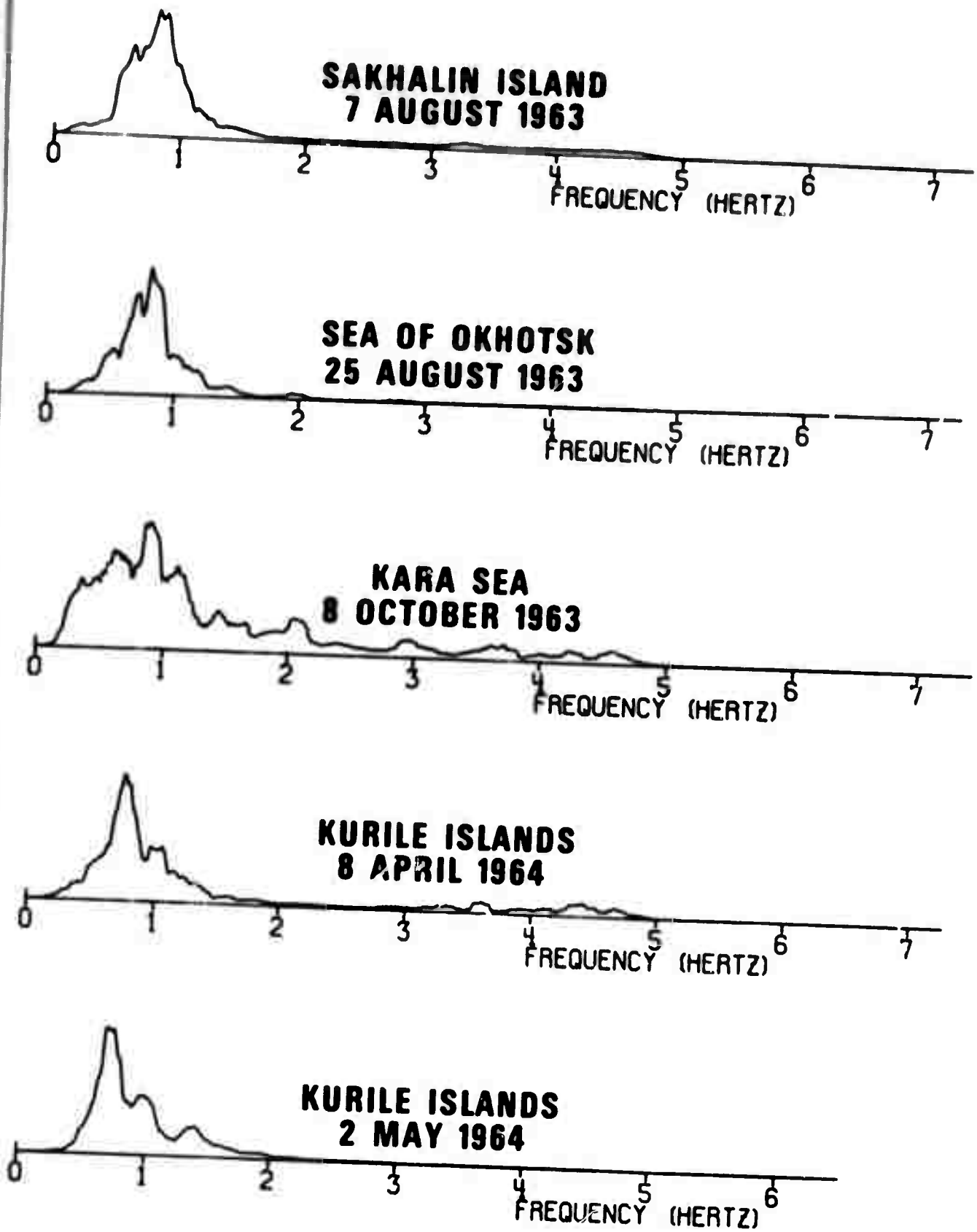

Figure 3. Earthquake spectra network sums.

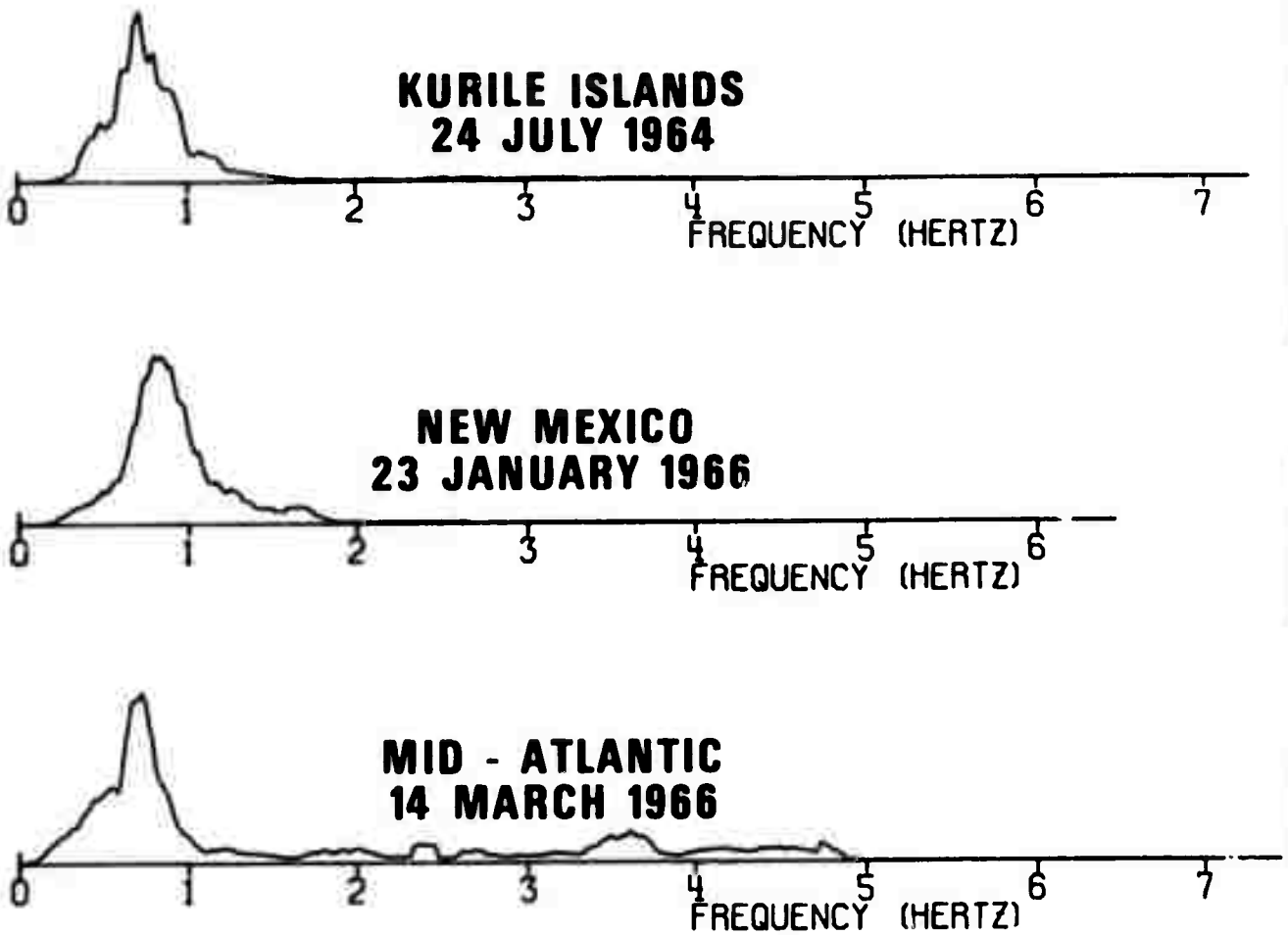

Figure 4. Earthquake spectra network sums.